On Hydraulic Constraints in Control of District Heating Systems

Agner, Felix

2023

Document Version:
Publisher's PDF, also known as Version of record

On Hydraulic Constraints in Control of District Heating Systems

Felix Agner

LUND
UNIVERSITY

Department of Automatic Control

Licentiate Thesis TFRT-3279
ISSN 0280–5316

Department of Automatic Control
Lund University
Box 118
SE-221 00 LUND
Sweden

Printed in Sweden by Media-Tryck.
Lund 2023

Abstract

District heating systems make an important puzzle piece in the energy system of both today and tomorrow. When designing, simulating and controlling these systems, hydraulics play a vital role. The pressure generated by pumps has to drive sufficient flow throughout the system to satisfy the requirements of customers. Ensuring that the system is sufficiently pressurized is a challenging task already in current systems, and may become even more challenging in the transition to the 4th generation of district heating.

In the first paper of this thesis, a demand response framework is suggested, which distributes the available flow to customers in a fair way. The framework aims to make it so that when the available pressure in the network is low, the buildings in the periphery should still be able to satisfy their heating needs.

The second paper of this thesis extends previous methods for identifying grey-box parameters for hydraulic district heating models. Previous methods of this type rely on more measurement points, and do not include the influence of the control valves situated in customer substations. These model parameters can then be used for simulation or control purposes.

Together, the results presented in this thesis provide tools for better dealing with the hydraulic limitations in district heating systems. At the end, future work is outlined which may further pave the way for improved control that takes hydraulic limitations into account.

Acknowledgements

First of all a big thank you to my supervisors. Thank you Anders for not only supporting me in research with valuable advice and input, but also for letting me find and follow problems that I find intrinsically motivating. Thank you Richard for often finding ways of looking at or presenting my problems and results from new points of view, often making things much more clear. Last but not least, thank you Pauline for being the one who without a doubt have been most engaged in the nitty-gritty of my work, helping me massively improve on details and formulations.

An equally large thanks goes out to the department of automatic control as a whole. I've heard many alumni say that this was the best work-place they ever had, and I can absolutely see why. The professional and social exchange with my fellow PhD-students has been great. And we would not have had half as good of a department were it not for the amazing work from our administrative staff.

Finally a huge thanks to Frida, my mom and my dad, for all your love and support.

This work is funded by the European Research Council (ERC) under the European Union's Horizon 2020 research and innovation program under grant agreement No 834142 (ScalableControl).

Contents

1

Introduction

1.1 Background

District heating systems play an important role in the energy systems of many countries. In 2016, 90 percent of energy use in Swedish multi-family dwellings was district heating [Energimyndigheten, 2017].

A traditional district heating system is illustrated in Figure 1.1. Cold water (between around 40 to 60 degrees, depending on the system) from the return pipeline is heated at production sites to a higher temperature (often to above 80 degrees, once again depending on the system). Large distribution pumps are then used to pump the now hot water through the supply lines out to consumers. The differential pressure generated by these pumps is what drives the flow of water. Consumers are connected to the network through *substations*. At these substations, the water in the internal hydraulic system of each building is heated through a heat exchanger, utilizing the hot water from the district heating system. The secondary hydraulic circuits then lead to radiators for space heating, or to preparation of hot water. While there are many different types of substation architectures, the one described here is typical

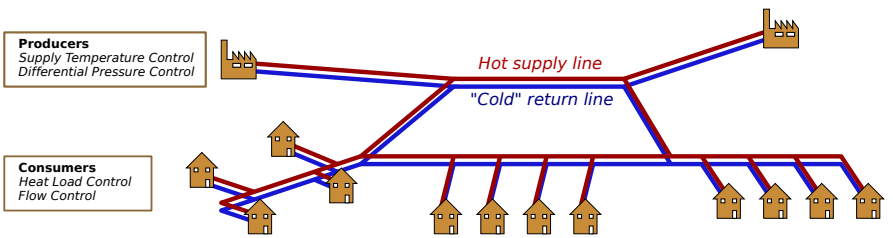

Figure 1.1 An overview of a traditional district heating system. At production sites, water from the less hot return line is heated, and pumped out through the hot supply line to reach consumers. At the production sites, the temperature of the water being pumped into the supply line, and the pressure generated by the pumps, are regulated in the *supply temperature* and *differential pressure* control loops. At consumption sites, the heat load is decided by the *head demand control*, and the amount of hot water to be pumped through the substation is given by the *flow control* loop.

in Sweden [Frederiksen and Werner, 2013]. In the substation, the side of the heat exchanger connected to the district heating network is called the *primary* side and the side connected to the interior hydraulic circuit is called the *secondary* side.

In the future, the approaching *4th generation* of district heating and cooling is expected to play an even more important role as a balancing force in the energy mix [Lund et al., 2014]. This new generation is characterized by, among other aspects, a *larger component of intermittent energy sources*, *lower supply temperatures*, *more interconnections with other parts of the energy system* and *more advanced control and measurement systems* [Lund et al., 2014; Lund et al., 2018].

1.2 Controlling District Heating Networks

Traditionally, district heating systems have been controlled by four independent control loops; *heat demand control*, *flow control*, *differential pressure control* and *supply temperature control* [Frederiksen and Werner, 2013; Vandermeulen et al., 2018]. The first two control loops are situated in customers' buildings. *Heat demand control* decides how much heat is used in the building, decided by domestic hot water usage, as well as radiator valve settings. *Flow control* decides the flow rate of hot water going through the primary side of the building's substation. This is generally performed by a control valve, which maintains a sufficiently high water temperature on the secondary side of the heat-exchanger. *Differential pressure control* and *supply temperature control* on the other hand are control loops controlled by the producer. In *differential pressure control*, the large pumps located at production sites are controlled such that the differential pressures in peripheral parts of the network are maintained at a high enough level that the flow control conducted by customers there should function. Lastly, *supply temperature control* decides the temperature of water supplied to the network.

The previously mentioned transition to the 4th generation of district heating comes with many challenges for controlling the system, such as the fluctuating nature of renewable energy sources, but also many possibilities such as smart meters with higher potential for measurements and communication [Vandermeulen et al., 2018]. There is plenty of academic literature focusing on analysis and design of control systems for this new generation. Some fields of research focus on stability and passivity properties of district heating networks [Machado et al., 2022; Strehle et al., 2022; Nørgaard Jensen et al., 2014]. These works have often focused on networks where each substation is fitted with an individual pump, an assumption which provides nice mathematical properties. There are also many works considering optimal control of single buildings, often considering an MPC-structured solution [Saletti et al., 2022; Frison et al., 2021]. Some works concern the optimization of production facilities. This thesis however is focused on coordinating a large number of consumers on the grid. While the control of the full grid is the subject of some works [Sandou et al., 2006; Saletti et al., 2021; Wang et al., 2017b], many of them work

under several limitations. They often do not take into account the constraints of hydraulic, but make the assumption that all flow rates are feasible. Another common limitation is the use of controller structures that rely heavily on centralized models and computations, imposing both strong assumptions on communication, real time computation, and central models and measurements. A final common assumption is that customer heat loads are a fixed constraint, which limits the possibility of increasing flexibility in the network by playing with this parameter.

1.3 The Importance of Hydraulic Constraints

In current generation district heating, a common occurrence is *bottlenecks* [Brange et al., 2019]. These bottlenecks occur when the flow rates in the network are large, causing significant pressure drops due to friction. The effect of this is that areas far away from pumps can experience a low pressure difference between supply and return lines [Frederiksen and Werner, 2013]. The differential pressure control cannot deal with this, because pumps are already working on full capacity, or cannot increase pressure further because it would cause problems closer to the pump. When this happens, the flow control loop fails as the valve does not have sufficient authority due to the differential pressure being too low. This means that even at full opening, the flow through the valve will not be sufficient. The consumer thus does not get the flow rate they require, and as a result, the building can become cold.

While this is a problem which already occurs in traditional district heating systems, it can potentially become even more important in the future. Two of the aforementioned changes when considering the transition to 4th generation district heating are *lower supply temperatures* and a *larger component of intermittent energy sources*. If existing networks are retrofitted for low supply temperatures, this might increase the issue of bottlenecks [Brange et al., 2019]. This is because if the supply temperature is lowered, some buildings may need to compensate for this reduction with a higher flow rate, which increases the pressure losses in the network. The inclusion of further intermittent energy sources may mean that certain producers at times may not be able to pump hot water into the grid, reducing pressure.

Understanding the hydraulic constraints of the system is not only important for bottlenecks. Pumping power is a significant aspect of the energy input to a district heating system, and models of the hydraulic constraints of the system can via improved control strategies reduce the required pumping effort [Wang et al., 2017b]. Such methods require model parameters describing the hydraulic characteristics of the grid. Some works have been published on estimating such model parameters [Wang et al., 2017a; Liu et al., 2020]. A limitation in these previously proposed methods is that they do not fully allow for control-related applications, as they do not incorporate the impact of valve settings in substations into the model. Another limitation is that they rely on the assumption of pressure measurements at every customer substation.

1.4 Problem Formulation

This thesis tackles two problems. The first problem is designing a control strategy for coordinating flow rates in a district heating system in order make the distribution of heat in the case of bottlenecks more fair. This means that the ability of peripheral consumers to keep their buildings warm should be similar to those close to production facilities. The second problem is extending previous hydraulic parameter identification methods to allow for fewer points of measurements and including estimation of parameters related to consumers control valves.

2

Theory

2.1 Distribution Grid Hydraulics

The topic of this thesis is tackling hydraulic constraints in district heating. Therefore a short introduction to the mathematical description of these constraints and their underlying assumptions is presented here.

While the hydraulics of district heating networks are dynamic in nature, as treated in parts of the control literature [Nørgaard Jensen et al., 2014; Machado et al., 2022; Strehle et al., 2022], these dynamics are much faster than those which govern the temperatures in the system [Frederiksen and Werner, 2013]. An often used approach when modeling and controlling temperature dynamics in a district heating network is to assume stationary hydraulic relationships, which is the approach considered in this thesis.

A district heating system can be regarded as a graph of edges and nodes, where each edge is a different hydraulic component and each interconnection of edges is a node. Each edge e is associated with a flow rate q_e, and each node i is associated with a pressure value p_i. This thesis concerns networks built from three types of components; *pipes, valves and pumps*. A very important concept for the later results, is that under certain assumptions (which will soon be covered), the static relation between these pressures and flows can be described as follows. Given a pipe or valve e leading from node i to node j, the difference in pressure p between nodes i and j can be given through the following relation:

$$p_i - p_j = s_e q_e |q_e| \tag{2.1}$$

where s_e is a hydraulic resistance parameter describing this relationship (In Paper I, the notation a_e was used instead of s_e). For valves, this parameter changes with the valve opening and for pipes it is constant. In paper I, these parameters are assumed given and are used to compute optimal, feasible flow rates in the network. In paper II, they are assumed unknown and to be estimated from data. The physical motivation behind (2.1) is as follows. For a pipe, the pressure-flow relationship can be

described by the Darcy-Weisbach equation:

$$p_i - p_j = q_e|q_e| \cdot \frac{2 f_{d,e} \rho L}{\pi^2 D_e^5}, \tag{2.2}$$

where q_e is the volumetric flow rate of water through the pipe, D_e is the diameter of the pipe, ρ is the density of the water, L is the length of the pipe and $f_{d,e}$ is the Darcy friction factor. In practice, this factor varies slightly with the flow rate of the water. However, in this thesis it is assumed constant. This assumption is based on both the fact that the factor becomes almost constant at high flow rates [Frederiksen and Werner, 2013] which is the case under bottleneck scenarios. It is also a commonly made assumption in simulation and modeling of district heating networks, such as for instance [van der Heijde et al., 2017a]. The pressure-flow relations for valves can be given as

$$p_i - p_j = q_e|q_e| \cdot \frac{1}{k_{vs}^2}, \tag{2.3}$$

where k_{vs} is the flow coefficient of the valve [Frederiksen and Werner, 2013]. This coefficient varies with the valve opening, and can have different characteristics. In this thesis, valves are assumed to be dimensioned to have a linear relationship between valve opening and k_{vs}. This means that the valve relation between flow and pressure can also be written on the form (2.1), where now s_e is dependent on the valve opening, and can vary between infinity (fully closed valve) and some minimum value (fully open valve). In Paper II, this linear relationship is expressed as $k_{vs} = u_e k_v$, where u_e is the opening level of the valve (between 0 and 1) and k_v is a linear factor. Valves do not necessarily have linear characteristics as is assumed here. The valves are often chosen to match the dimension of the connected heat exchanger. However, in district heating substations these heat exchangers are often generously dimensioned such that a linear relation is sensible [Frederiksen and Werner, 2013].

Lastly for pumps, the relation is modeled with a *pump head curve*, which changes depending on the operating frequency of the pump [Wang et al., 2017b]. For a pump e, this relation can be given by

$$p_i - p_j = c_1 q_e|q_e| + c_2 r_e + c_3 r_e^2 \tag{2.4}$$

where c_1, c_2 and c_3 are given parameters and r_e is the relative pump frequency of the pump, bounded by 1. An important implication of this curve is that there is an upper limit to the differential pressure which can be provided by the pump.

When analyzing the full network and not just a single edge, another assumption is made, which is that the network is a closed hydraulic circuit. This means that for each node, the amount of water entering the node from connected edges is equal to the amount of water leaving. This is an important concept which is used in both paper I and paper II to analyze the properties of the grid.

2.2 Thermodynamic Building Models

Paper I concerns not only the hydraulic behavior of the grid, but also building thermodynamics. Therefore a quick overview of building thermodynamics modeling in general and the model used in paper I in particular is provided here. A common approach to modeling thermodynamics in buildings is through the use of *RC-models*. These models play a thermodynamics counterpart to electrical circuits composed of resistors and capacitors. In the thermodynamics version, capacitors represent thermal mass, such as walls and air in rooms. Resistors represent heat transmission between these thermal masses. The resistances represent a lumped representation of heat transfer in the form of both conductance, convection and radiation (where the nonlinear parts of the latter are assumed negligible) [Frahm et al., 2022]. In modeling and control of buildings, one can find numerous examples of this type of model being employed [Bacher and Madsen, 2011; Saletti et al., 2022; Frahm et al., 2022; van der Heijde et al., 2017b]. Depending on the application, one can establish models of varying complexity, ranging from modeling the temperature in individual walls, radiators and rooms [Bacher and Madsen, 2011] to lumping the thermal energy of the entire building into one state [Saletti et al., 2022].

This thesis concerns the analysis of a large number of buildings, rather than detailed understanding of a single building. Therefore a simple RC-model framework has been used. Each building is modeled with two temperature states, T_{in} and T_{hs}, representing the temperatures in the building interior and the radiator system respectively. The indoor temperature T_{in} is the variable which best defines the notion of fair distribution of heat and is as such included in the model. The radiator system temperature T_{hs} is included as it is a crucial part of traditional heat load control and flow control, a structure which this thesis strives to maintain and improve upon.

The following equations, which can be found in Paper I, represent the dynamics for one building.

$$C_{\text{in}}\dot{T}_{\text{in}} = \frac{1}{R_{\text{ext}}}\left(T_{\text{ext}} - T_{\text{in}}\right) + \frac{1}{R_{\text{hs}}}\left(T_{\text{hs}} - T_{\text{in}}\right) \tag{2.5}$$

$$C_{\text{hs}}\dot{T}_{\text{hs}} = \frac{1}{R_{\text{hs}}}\left(T_{\text{in}} - T_{\text{hs}}\right) + P. \tag{2.6}$$

Here R_{ext} and R_{hs} represent the thermal resistance between the building interior and exterior, and the building interior and heating system respectively. C_{in} and C_{hs} are the thermal capacitances of the building interior and heating system. P is the heat load of the building, i.e. the heat which is taken from the district heating system and transferred through a heat exchanger to the building heating system. T_{ext} is the outdoor temperature.

The heat load P is given by

$$P = C_w(T_{\text{sup}} - T_{\text{ret}})q \tag{2.7}$$

where C_w is the specific heat capacity of water, T_{sup} and T_{ret} are the supply-and-return temperatures on the primary side of the substation, and q is the volume flow rate. The relation between P and q is in general not linear, and the level of non-linearity varies with the sizing of the heat exchanger [Benonysson and Boysen, 1996]. In practice, this means that the difference between supply temperature T_{sup} and return temperature T_{ret} varies with the volume flow rate. However, substation heat exchangers are often generously sized, making the relationship close to linear [Frederiksen and Werner, 2013], which is the assumption maintained in this thesis.

3

Contributions

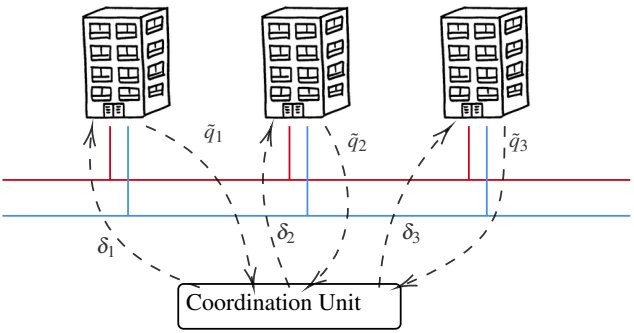

Figure 3.1 A sketch of the demand response method proposed in paper I. Each building i locally calculates a desired flow rate $\tilde{q}_i$, which is treated by a central coordination unit. The central unit calculates a reduction δ_i for each unit which should lead to a more fair distribution of heat.

3.1 Paper I

This journal paper presents a demand response method for ensuring a more fair distribution of flow rates in a district heating network. A sketch of the method is shown in Figure 3.1. Each building is responsible for locally calculating a desired flow rate corresponding to a classical uncoordinated case. A central unit gives each building a reduction in flow rate which should make the distribution more fair. In the paper, the hydraulic resistance parameters of equation (2.1) are used to find a convex description of possible flows rates. The central unit then solves a convex optimization problem over this set of possible flows. The method is evaluated on a numerical example, constituting a proof-of concept that methods of this type can alleviate the effect of hydraulic bottlenecks in district heating systems.

The contributions of the author of this thesis are modeling, formulating the proposed coordination method, simulation and writing the majority of the paper.

3.2 Paper II

Control strategies which explicitly account for hydraulic constraints, such as the method proposed in Paper I, require the parameters s_i as presented in (2.1) to be known. Paper II considers the problem of estimating these parameters from data in a branched district heating network. This is done by analyzing the flow constraints in the network, which allows formulating a linear relationship between the hydraulic resistance parameters and measured pressures in the network. This relationship can then be used to fit the parameters s_i which best match the observed data, which in Paper II is done through a simple least-squares solution. This conference paper extends previous work on the topic by considering parameterization of control valves, which is a crucial contribution for control purposes. In addition, the paper shows that even when using much fewer measurements of pressure than previously investigated, the hydraulic resistance parameters of the system can in theory be uniquely determined.

The author of this thesis contributed to the work through establishing the theoretical results, performing numerical examples and writing.

4

Discussion

4.1 Conclusions

This thesis concerns a two-fold contribution. The first contribution concerns a control strategy for coordinating the flow rates in a district heating system so as to reduce the impact of hydraulic bottlenecks on the comfort temperatures in peripheral buildings. The proposed strategy contains several simplifying assumptions, such as constant supply temperatures in the grid, proportional controllers in buildings, and simplified building dynamics. However, through a proof of concept simulation it is shown that the method reduces the worst-case temperature deviations caused by bottlenecks. This is done with a method which is light-weight, and requires the central coordinating unit to have minimal information about the underlying states and models of buildings.

The second contribution concerns the identification of hydraulic model parameters for use in simulations and control strategies, such as the first contribution. The work shows that parameters can be uniquely determined using fewer data points than shown previously in the literature, and extends previous work to include the impact of substation control valves which is an important factor for control applications. The method rests on the assumption of linear valve characteristics and available data of valve set-points.

4.2 Ethics

It is an important part of research to reflect upon the ethics of ones work, and in fact it is even a mandatory aspect of the doctoral student education in Sweden. As such, this section will cover a short discussion on the ethical implications of the research conducted in this thesis.

Paper I covers the development of a *demand response* method, specifically under the category of *direct load control*. This is a field of research in the energy sector, most often carried out in power systems, where the demand side of the energy balance is adjusted [O'Connell et al., 2014; Guelpa and Verda, 2021]. The ethical

implications of Paper I fall under the larger umbrella of ethical implications related to demand response and direct load control research. A comprehensive study of ethical concerns in this field from the perspective of energy justice was performed in [Calver and Simcock, 2021]. Some of the concerns highlighted in this work apply to paper I. To begin with the positive aspects, demand response is often highlighted as a way of potentially introducing more renewable energy into the energy mix. This holds also for Paper I. The increased robustness to insufficient pressure that the approach of Paper I provides could mean that a grid operator can introduce more fluctuating (renewable) energy sources. This is because temporary reductions in the energy supplied to the grid will have a less severe impact on the connected buildings than it would otherwise. This would provide a climate-positive effect, which is a positive ethical aspect. However, a concern that one can raise with regards to the proposed method is the amount of power and influence over the energy market that is placed in the hands of the operator. The proposed approach implies that a district heating operator should have a direct influence on the heat load of consumers, and without a solid legal framework there is no guarantee that this power will be used ethically. An operator could for instance save money by constructing a poorly dimensioned grid, and assume that the proposed load control will ensure that none of the connected consumers become too disgruntled with the poor quality of energy supply.

Paper II concerns the processing of domestic heat load data. As this is data connected to the behavior of individuals, it should be subject to some scrutiny. However, the proposed methodology does not deal in identifying the behavior or characteristics of individual persons. Rather it mainly focuses on modeling the network outside the domain of the buildings. In fact, the consumer data which is necessary for the method consists of only two measurements; *volume flow rates* and *valve set-points*. Volume flow rates are already used for invoicing [Frederiksen and Werner, 2013] and as such does not further invade privacy. Valve set-points are outside the scope of regular invoicing, however, it is hard to motivate that this additional metric should further implicate the privacy of customers.

4.3 Outlooks and Future Work

There are several open challenges with regards to the challenges tackled by both Paper I and Paper II.

Considering Paper II, the robustness of the method when subject to real, or more realistic data, should be evaluated. Another open area is that recent results on the field [Liu et al., 2020; Yin et al., 2018] take only tree-shaped networks into account, or solve the meshed network problem by iteratively sealing off parts of the network so that in each identification step the graph forms a tree. Many of the nice mathematical properties that come with the tree-shaped nature of the networks disappear when taking loops into account.

Concerning Paper I, the problem of coordinating flow rates in district heating systems has several open ends. One direction to take the work is taking steps towards applicability in real world systems by accounting for more advanced consumer controllers and considering robustness to model errors and simplifications. One could also consider adding predictive behaviour into the system, so as to have the coordination unit anticipate periods where bottlenecks occur, and act accordingly. Another approach is to generalize the work to further emphasize the control-theoretical aspects. A number of independent agents sharing a common resource is not a unique problem to district heating systems. For instance, it has parallels in the optimal power flow problem in power systems [Dall'Anese and Simonetto, 2018] as well as allocating message frequency in the transmission control protocol (TCP) [Low et al., 2002; Kelly, 2003]. Therefore, generalizing the problem into a broader framework can present opportunities to both learn from and contribute to other fields of application.

Bibliography

Bacher, P. and H. Madsen (2011). "Identifying suitable models for the heat dynamics of buildings". en. *Energy and Buildings* **43**:7, pp. 1511–1522. ISSN: 03787788. DOI: 10.1016/j.enbuild.2011.02.005. URL: https://linkinghub.elsevier.com/retrieve/pii/S0378778811000491 (visited on 2021-07-14).

Benonysson, A. and H. Boysen (1996). "Optimum control of heat exchangers". **25**. Presented at 5th International Symposium on Automation of District Heating systems, Finland, August 1995, pp. 496–504.

Brange, L., K. Sernhed, and M. Thern (2019). "Decision-making process for addressing bottleneck problems in district heating networks". en. *International Journal of Sustainable Energy Planning and Management* **20**, pp. 37–50.

Calver, P. and N. Simcock (2021). "Demand response and energy justice: a critical overview of ethical risks and opportunities within digital, decentralised, and decarbonised futures". *Energy Policy* **151**, p. 112198. ISSN: 0301-4215. DOI: https://doi.org/10.1016/j.enpol.2021.112198. URL: https://www.sciencedirect.com/science/article/pii/S0301421521000677.

Dall'Anese, E. and A. Simonetto (2018). "Optimal power flow pursuit". *IEEE Transactions on Smart Grid* **9**:2, pp. 942–952. DOI: 10.1109/TSG.2016.2571982.

Energimyndigheten (2017). *Summary of energy statistics for dwellings and nonresidential premises for 2016*. Tech. rep. Statens energimyndighet. URL: https://www.energimyndigheten.se/49abd2/globalassets/statistik/officiell-statistik/statistikprodukter/energistatistik-i-smh-fbhlok/rapporter/energistatistik-for-smahus-flerbostadshus-och-lokaler-2016.pdf.

Frahm, M., F. Langner, P. Zwickel, J. Matthes, R. Mikut, and V. Hagenmeyer (2022). "How to derive and implement a minimalistic rc model from thermodynamics for the control of thermal parameters for assuring thermal comfort in buildings." *2022 Open Source Modelling and Simulation of Energy Systems*

(OSMSES), Open Source Modelling and Simulation of Energy Systems (OSMSES), 2022, pp. 1–6. ISSN: 978-1-6654-1008-3. URL: https://ludwig.lub.lu.se/login?url=https://search.ebscohost.com/login.aspx?direct=true&AuthType=ip,uid&db=edseee&AN=edseee.9769134&site=eds-live&scope=site.

Frederiksen, S. and S. Werner (2013). *District heating and cooling*. Studentlitteratur. Chap. 2.

Frison, L., A. Oliva, and S. Herkel (2021). "Mpc for collaborative heat transfer in a district heating network with distributed renewable energy generation and storage". In: *2021 European Control Conference (ECC)*, pp. 1669–1674. DOI: 10.23919/ECC54610.2021.9655041.

Guelpa, E. and V. Verda (2021). "Demand response and other demand side management techniques for district heating: A review". en. *Energy* **219**. ISSN: 03605442. DOI: 10.1016/j.energy.2020.119440. URL: https://linkinghub.elsevier.com/retrieve/pii/S0360544220325470.

Kelly, F. (2003). "Fairness and stability of end-to-end congestion control*". *European Journal of Control* **9**:2, pp. 159–176. ISSN: 0947-3580. DOI: https://doi.org/10.3166/ejc.9.159-176. URL: https://www.sciencedirect.com/science/article/pii/S0947358003702738.

Liu, Y., P. Wang, and P. Luo (2020). "Pipe hydraulic resistances identification of district heating networks based on matrix analysis". *Energies* **13**:11. ISSN: 1996-1073. DOI: 10.3390/en13113007.

Low, S., F. Paganini, and J. Doyle (2002). "Internet congestion control". *IEEE Control Systems Magazine* **22**:1, pp. 28–43. DOI: 10.1109/37.980245.

Lund, H., P. A. Østergaard, M. Chang, S. Werner, S. Svendsen, P. Sorknæs, J. E. Thorsen, F. Hvelplund, B. O. G. Mortensen, B. V. Mathiesen, C. Bojesen, N. Duic, X. Zhang, and B. Möller (2018). "The status of 4th generation district heating: research and results". *Energy* **164**, pp. 147–159. ISSN: 0360-5442. DOI: https://doi.org/10.1016/j.energy.2018.08.206.

Lund, H., S. Werner, R. Wiltshire, S. Svendsen, J. Thorsen, F. Hvelplund, and B. Mathiesen (2014). "4th generation district heating (4GDH)". *Energy* **68**, pp. 1–11. ISSN: 03605442. DOI: 10.1016/j.energy.2014.02.089. URL: https://linkinghub.elsevier.com/retrieve/pii/S0360544214002369 (visited on 2021-07-14).

Machado, J. E., M. Cucuzzella, and J. M. Scherpen (2022). "Modeling and passivity properties of multi-producer district heating systems". *Automatica* **142**, p. 110397. ISSN: 0005-1098. DOI: https://doi.org/10.1016/j.automatica.2022.110397. URL: https://www.sciencedirect.com/science/article/pii/S0005109822002503.

Nørgaard Jensen, T., R. Wisniewski, C. DePersis, and C. Skovmose Kallesøe (2014). "Output regulation of large-scale hydraulic networks with minimal steady state power consumption". *Control Engineering Practice* **22**, pp. 103–113. ISSN: 0967-0661. DOI: https://doi.org/10.1016/j.conengprac.2013.10.004. URL: https://www.sciencedirect.com/science/article/pii/S096706611300186X.

O'Connell, N., P. Pinson, H. Madsen, and M. O'Malley (2014). "Benefits and challenges of electrical demand response: a critical review". *Renewable and Sustainable Energy Reviews* **39**, pp. 686–699. ISSN: 1364-0321. DOI: https://doi.org/10.1016/j.rser.2014.07.098. URL: https://www.sciencedirect.com/science/article/pii/S1364032114005504.

Saletti, C., N. Zimmerman, M. Morini, K. Kyprianidis, and A. Gambarotta (2021). "Enabling smart control by optimally managing the state of charge of district heating networks". *Applied Energy* **283**, p. 116286. ISSN: 0306-2619. DOI: https://doi.org/10.1016/j.apenergy.2020.116286. URL: https://www.sciencedirect.com/science/article/pii/S0306261920316743.

Saletti, C., N. Zimmerman, M. Morini, K. Kyprianidis, and A. Gambarotta (2022). "A control-oriented scalable model for demand side management in district heating aggregated communities". *Applied Thermal Engineering* **201**, p. 117681. ISSN: 1359-4311. DOI: https://doi.org/10.1016/j.applthermaleng.2021.117681. URL: https://www.sciencedirect.com/science/article/pii/S1359431121011066.

Sandou, G., S. Font, S. Tebbani, A. Hiret, and C. Mondon (2006). "Predictive control of a complex district heating network". In: vol. 2005, pp. 7372–7377. DOI: 10.1109/CDC.2005.1583351.

Strehle, F., J. Machado, M. Cucuzzella, A. Malan, J. Scherpen, and S. Hohmann (2022). "Port-hamiltonian modeling of hydraulics in 4th generation district heating networks". In: pp. 1182–1189. DOI: 10.1109/CDC51059.2022.9992887.

van der Heijde, B., M. Fuchs, C. Ribas Tugores, G. Schweiger, K. Sartor, D. Basciotti, D. Müller, C. Nytsch-Geusen, M. Wetter, and L. Helsen (2017a). "Dynamic equation-based thermo-hydraulic pipe model for district heating and cooling systems". *Energy Conversion and Management* **151**, pp. 158–169. ISSN: 0196-8904. DOI: https://doi.org/10.1016/j.enconman.2017.08.072. URL: https://www.sciencedirect.com/science/article/pii/S0196890417307975.

van der Heijde, B., M. Sourbron, F. Vega Arance, R. Salenbien, and L. Helsen (2017b). "Unlocking flexibility by exploiting the thermal capacity of concrete core activation". *Energy Procedia* **135**. 11th International Renewable Energy Storage Conference, IRES 2017, 14-16 March 2017, Düsseldorf, Germany, pp. 92–104. ISSN: 1876-6102. DOI: https://doi.org/10.1016/j.egypro.

2017.09.490. URL: https://www.sciencedirect.com/science/article/pii/S1876610217345939.

Vandermeulen, A., B. van der Heijde, and L. Helsen (2018). "Controlling district heating and cooling networks to unlock flexibility: A review". en. *Energy* **151**, pp. 103–115. ISSN: 03605442. DOI: 10.1016/j.energy.2018.03.034. URL: https://linkinghub.elsevier.com/retrieve/pii/S0360544218304328 (visited on 2021-07-14).

Wang, N., S. You, W. Zheng, H. Zhang, X. Zheng, and T. Ye (2017a). "A simple thermal dynamics model and parameter identification of district heating network". *Procedia Engineering* **205**. 10th International Symposium on Heating, Ventilation and Air Conditioning, ISHVAC2017, 19-22 October 2017, Jinan, China, pp. 329–336. ISSN: 1877-7058. DOI: https://doi.org/10.1016/j.proeng.2017.09.988.

Wang, Y., S. You, H. Zhang, W. Zheng, X. Zheng, and Q. Miao (2017b). "Hydraulic performance optimization of meshed district heating network with multiple heat sources". *Energy* **126**, pp. 603–621. DOI: 10.1016/j.energy.2017.03.044.

Yin, G., B. Wang, T. Sheng, H. Sun, Q. Guo, and Z. Qiao (2018). "Network parameter estimation for district heating system". In: *2018 2nd IEEE Conference on Energy Internet and Energy System Integration (EI2)*, pp. 1–6. DOI: 10.1109/EI2.2018.8582515.

Paper I

Combating District Heating Bottlenecks Using Load Control

Felix Agner Pauline Kergus Richard Pates Anders Rantzer

Abstract

The 4th generation of district heating systems face a potential problem where lowered water temperatures lead to higher flow rates, which requires higher hydraulic capacity in terms of pipe and pump sizes. This increases the effect of the already existing issue of hydraulic bottlenecks, causing peripheral units (customers) to experience reduced flow rates. A coordinating control strategy is presented in this work aimed at reducing the effect of such bottlenecks on the comfort of customers. This is done by distributing the flow deficit over many units rather than a few. Previous works mainly focus on MPC-structured controllers that depend on complex system models and online optimization techniques. This work proposes a method that requires little information about models for individual units and minimal IT communication between control systems. The proposed method is compared with a traditional control strategy and an optimal baseline in a simulation study. This shows that the proposed method can decrease the worst case indoor temperature deviations.

Originally published in Smart Energy. Reprinted with permission.

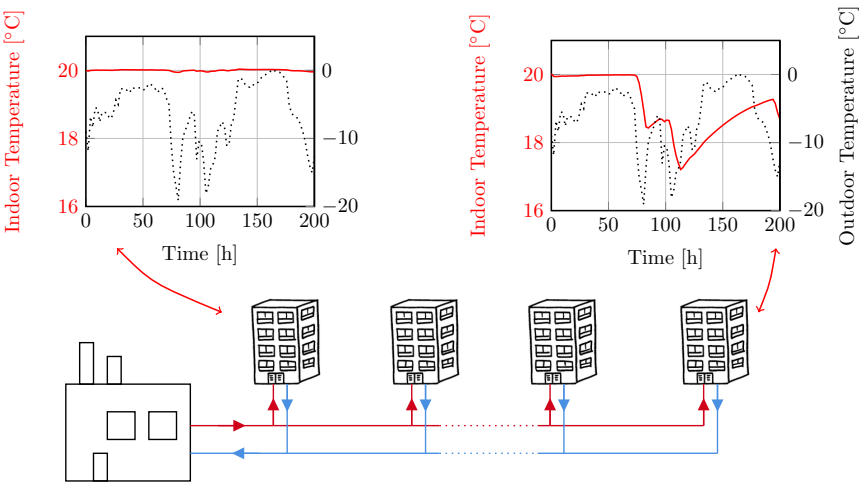

Figure 1. Discrepancy in indoor temperature (red) between units connected to the grid. When the outdoor temperature (dotted) becomes critically cold, units close to the pressure source are able to maintain indoor comfort temperature while units far from the source are not.

1. Introduction

One important puzzle piece of the smart energy system of the future is the integration of a variety of energy sources and distribution methods. This allows harnessing synergies and reducing the impact of stochastic fluctuations in energy supply and demand [Mathiesen et al., 2015]. District heating systems have been shown to be a powerful tool in this energy system, but research indicates that a transformation of district heating from the old 3rd generation to a new 4th generation is needed. An important characteristic of this emerging 4th generation that allows it to be integrated into the overall energy chain is reduced supply water temperatures which would allow using previously untapped heat sources such as renewable sources and industrial waste heat [Lund et al., 2014]. In theory, the reduction in supply temperature should be accompanied by an equal drop in return temperature, leading to an equal temperature difference and thus no alternation in the necessary flow [Lund et al., 2018]. However, lowering the building return temperatures requires an improvement in space heating technology [Lund et al., 2017], [Lund et al., 2018] and if such is not the case there may be a reduction in differential temperature. This leads to higher flows needed to distribute the same amount of power, implying that the piping and pumping power of 4th generation district heating systems may have to be dimensioned for higher capacity. This presents an additional cost. It also reduces the potential of retrofitting existing infrastructure for lower grid temperatures, which otherwise may prove a cost-effective solution [Lund et al., 2018], [Brange

et al., 2019]. If the grid capacity is not dimensioned for higher flows, it may lead to **bottlenecks** [Brange et al., 2019].Bottlenecks imply that the pressure losses in part of the distribution grid are too high, leaving an insufficient differential pressure between supply and return pipes in subsequent parts of the network. This happens when the water flow is too great for the dimensions of the piping. Buildings (units) connected in these parts may find it hard to extract sufficient flows to keep indoor temperatures at comfort level. In fact, this is not only a hypothetical problem in future generations of district heating but is already a problem in currently operating networks [Frederiksen and Werner, 2013]. This phenomenon arises under **peak load conditions**, i.e. when the flows in the network are high, coinciding with when the outdoor temperature is low. Figure 1 shows this problem, based on simulation which will be explained later in this article. When the outdoor temperature becomes too low, the indoor temperatures start to differ from each other. Buildings close to the pressure source maintain comfort temperature while it becomes cold in buildings further down the distribution line. Reducing the effect of bottlenecks could increase **robustness** to low outdoor temperatures, in the sense that a drop in outdoor temperature would cause reduced worst-case deviations in indoor temperature. Apart from the possibility of reducing supply temperatures, this could also grant the possibility of extending existing networks, and designing larger new networks with less concern for critical outdoor temperature and the influence this would have on customer comfort. One approach to tackling this issue is through the use of demand side management, as suggested in [Frederiksen and Werner, 2013] [Vandermeulen et al., 2018] [Brange et al., 2019] [Guelpa and Verda, 2021].

Demand side management is an umbrella term for different ways of altering the demand of customers connected to a grid. There is a rich history of demand side management in the power grid literature, but it has also begun making an appearance in the district heating literature [Guelpa and Verda, 2021]. This article focuses specifically on direct load control, i.e. directly altering and deciding the heat load of customers. A common approach to direct load control is to use **centralized** optimization with the objective of minimizing some operational cost for the entire network. For instance an optimization scheme was introduced in [Bhattacharya et al., 2019] to improve fairness of heat distribution in a line network. As the optimization problems tend to grow drastically with the number of connected units, these methods can run into problems of scalability. Another approach is to have **decentralized** optimal controllers, such as in [Saletti et al., 2020], and then combine their signals to compute desired heat production. However in this scenario there is no coordination between the different units to ensure that they request a load that is feasible.

To ensure that any enacted heat loads are within the system constraints, a good model of the grid is needed. In practice, the considered distribution model depends on the purpose of the model as well as the design of the network, as summarized in

[Sarbu et al., 2019]. Some works choose to disregard aspects of the constraints given by the network such as pressure losses or time delays [Bhattacharya et al., 2019]. One common approach to model flows and pressures of the network is to assume that the specific heat load at each unit has to be met, and then using these loads to calculate the flows realized in the network [Wang et al., 2017], [Benonysson et al., 1995], [Larsen et al., 2002]. However this approach does not hold in the case where the desired heat loads of each building cannot be met due to the corresponding flows being too large for the network to handle. To the authors' knowledge, there is little work on describing the limits on the flows in the system.

This work is focused on understanding how bottlenecks can be combated through direct load control, in such a way that the hydraulic constraints of the network are taken into account and the control structure remains scalable for a large number of connected units. The idea is to combine the increased ease of implementation of distributed controllers with the system-level benefits of a centralized strategy. An important distinction to make is that many works on demand side management try to optimize some operational cost, e.g. cost of energy production units. In this work we assume that the system operates at full capacity, and the objective is simply to distribute the supplied energy fairly between customers.

The contribution of this work is in three parts;

1. formulating the constraints limiting the unit flows in a line-structured district heating grid;
2. introducing a load coordination scheme that builds on the traditional control architecture of district heating such that it should be easy to implement in existing networks, and;
3. comparing two control architectures; traditional control and the aforementioned load coordination architecture, with an optimal baseline reference through a simulation study.

The work is presented as follows: Section 3.1 introduces a mathematical formulation of the problem. The notion of robustness to outdoor temperatures is introduced here. Section 3 presents the mathematical models of the network and the units connected to the network. Section 4 defines two different control architectures and an optimal baseline reference, which are then compared in a simulation study described in section 5. The results and future work are finally discussed in section 6.

2. List of Notation

Table 1 lists the notation used in this article. In addition to this table, three other conventions are used:

- Vectors are noted with bold face, e.g. $\mathbf{q}$ denotes a vector of flows.
- Indices are used to reference elements of a vector or matrix. If the vector notation already contains subset notation, these are separated by a comma. For instance, $T_{c,i}$ refers to element i in the vector of comfort temperatures $\mathbf{T}_c$. M_{ij} refers to matrix element of row index i, column index j.

Table 1. Table of notation used in this article.

Symbol	Description	Unit
J	Cost function related to discomfort	°Cs
T	Temperature	°C
T_c	Comfort temperature	°C
T_{in}	Indoor temperature	°C
e	Difference between indoor and comfort temperature	°C
T_{hs}	Temperature of water in heating system	°C
T_{ext}	Outdoor temperature	°C
T_{sup}	Primary side supply temperature	°C
T_{ret}	Primary side return temperature	°C
t	Time	s
t_s	Sampling time	s
q	Water flow	kg/s
$\mathcal{Q}$	The set of admissible system water flows	-
C_{in}	Heat capacity of indoor area	J/°C
C_{hs}	Heat capacity of water in radiator systems	J/°C
C_w	Specific heat capacity of water	J/kg°C
R_{ext}	Heat resistance between building interior and exterior	°C/W
R_{hs}	Heat resistance between radiator system and building interior	°C/W
P	Furnished heat power	
A, B_q, B_{ext}	Matrices defining the dynamics of simulated buildings	-
Δp	Differential pressure	Pa
$\mathcal{L}$	Network loop	-
F	Network incidence matrix	-
a	Hydraulic resistance	Pa/(kg/s)^2
c	Pump curve parameters	-
r	Pump frequency ratio	-
α_0,α_1	Heating system temperature set-point parameters	-
k	Building P-controller gain	kg/s°C
δ	Flow set-point deviation	kg/s
γ	Coordination weight factor	s°C/kg
λ	Coordination price factor	-

3. Problem and System Formulation

This section formalizes the problem of this work. Part 3.1 puts the problem to be solved in mathematical form. Part 3.2 presents the model of building temperature dynamics and the union between buildings and the district heating grid. Part 3.3

explains the hydraulic model of the distribution network, dictating the constraints on hot water flow in the system. Formulating these constraints in closed form constitutes the first contribution of the article.

3.1 Problem Formulation

The control problem of this work is to maintain comfortable indoor temperatures in all buildings connected to a district heating network even under extreme disturbances in the form of low outdoor temperatures. The control signal deciding the amount of heat furnished to each building i is the flow of hot water q_i through their substation. Mathematically, the problem is formulated as:

$$\begin{aligned} \min_{\mathbf{q}(t_k)} \quad & J(\mathbf{T}) && \text{(1a)} \\ \text{subject to} \quad & \mathbf{T}(t_{k+1}) = f(\mathbf{T}(t_k), \mathbf{q}(t_k), T_{\text{ext}}(t_k)) && \text{(1b)} \\ & \mathbf{q}(t_k) \in \mathcal{Q}. && \text{(1c)} \end{aligned}$$

What this means is that we want to minimize some discomfort J related to the indoor temperatures $\mathbf{T}$ in the connected buildings. These temperatures $\mathbf{T}$ evolve according to dynamics f, which depend on the furnished flows $\mathbf{q}$ and the outdoor temperature T_{ext}. This relationship f will be detailed in the next section, 3.2 and is in this work modelled linearly. Lastly, the furnished flow $\mathbf{q}$ is limited by the capacity of the distribution system. The set $\mathcal{Q}$ of flows that can be realized in the system is the subject of section 3.3.

The cost function J should capture the discomfort experienced by each customer. To define this discomfort, consider the temperature deviation $e_i(t_k)$ for each unit i connected to the grid at each point in time t_k. $e_i(t_k)$ is the deviation between the desired comfort temperature $T_{c,i}$ and the actual indoor temperature $T_{\text{in},i}(t_k)$.

$$e_i(t_k) = T_{c,i} - T_{\text{in},i}(t_k) \tag{2}$$

The discomfort J_i experienced by a unit during a time period $t = t_1, t_2, \ldots, t_K$ can then be defined as

$$J_i = \sum_{k=1}^{K} |e_i(t_k) t_s|, \tag{3}$$

where t_s is the time in between times t_k and t_{k+1}. Note also three candidates for

measuring the system-level discomfort, J_1, J_2 and J_∞:

$$J_1 = \sum_{k=0}^{K} \frac{1}{N} \sum_{i=1}^{N} |e_i(t_k)t_s| \tag{4}$$

$$J_2 = \sum_{k=0}^{K} \sqrt{\frac{1}{N^2} \sum_{i=1}^{N} |e_i(t_k)t_s|^2} \tag{5}$$

$$J_\infty = \sum_{k=0}^{K} \max_i(|e_i(t_k)t_s|) \tag{6}$$

Here J_1 is a metric for the sum of discomfort experienced by all units, J_2 is a metric for the total discomfort where larger units discomfort are penalized more, and J_∞ is a metric for the worst discomfort experienced in the grid. The scenario we want to avoid is for extreme discomfort levels to arise in any unit, and for this reason the J_∞-cost is the cost that will be used in the controller design of section 4. The two remaining costs, J_1 and J_2 will be used for evaluation as a point of reference.

REMARK 1
Some works also consider optimizing over the power required to actuate the flows and temperatures in the grid and thus minimize the cost of running the system. For instance [Saletti et al., 2020] consider the utilized pumping power and [Bacher and Madsen, 2011] consider the electrical heating power in an adjacent problem considering an electrically heated unit. In this work we don't consider the cost of running the system. As we are interested in fair distribution under extremely cold situations, it is assumed that the heat and pumping power supplied to the system will have to be at maximum capacity. The interest is rather in understanding how to distribute this supplied power between connected units.

3.2 Buildings

Here we investigate the dynamics dictating the temperatures in each building, i.e. the function f of (1b). With each building i, we associate two states $T_{\text{in},i}$ and $T_{\text{hs},i}$, representing the mean indoor temperature and mean temperature of heating system circulating water respectively. This allows the construction of the following state space representation:

$$C_{\text{in},i}\dot{T}_{\text{in},i} = -(\frac{1}{R_{\text{ext},i}} + \frac{1}{R_{\text{hs},i}})T_{\text{in},i} + \frac{1}{R_{\text{hs},i}}T_{\text{hs},i} + \frac{1}{R_{\text{ext},i}}T_{\text{ext}} \tag{7}$$

$$C_{\text{hs},i}\dot{T}_{\text{hs},i} = \frac{1}{R_{\text{hs},i}}T_{\text{in},i} - \frac{1}{R_{\text{hs},i}}T_{\text{hs},i} + P_i, \tag{8}$$

where $C_{\text{in},i}$ and $C_{\text{hs},i}$ is heat capacity of the building interior and heating system respectively. P_i is the heat power extracted from the primary side of the district heating

system. The heat energy flow between interior and exterior as well as between heating and system interior are proportional to the inverse of the heat resistances $R_{\text{ext},i}$ and $R_{\text{hs},i}$ respectively. These types of models of varying complexity have been used extensively in literature on modeling building temperature dynamics,[Bacher and Madsen, 2011], [Bhattacharya et al., 2019], [Saletti et al., 2020], and can be augmented to capture different levels of complexity. In this work, a simple model of buildings is used, motivated by the interest in understanding the general distribution of temperatures in a large set of buildings, rather than the details of one individual building. The presented continuous time state space representation can then be transformed into a discrete time representation of the system if a standard zero-order-hold assumption is made for the inputs T_{ext} and P_i.

The heat energy, P_i, extracted from the network is here assumed to be proportional to the water flow through the primary side pipes of the building substation and the temperature difference between supply and return pipes in the network, $(T_{\text{sup}} - T_{\text{ret}})$:

$$P_i = C_w(T_{\text{sup}} - T_{\text{ret}})q_i \tag{9}$$

where C_w is the specific heat capacity of water. In the simulations and analysis in this work, the supply and return temperatures in the network are considered constant. This simplification is made to simplify simulations and analysis. While these temperatures are not constant in a real system, they are measured in building substations. As such, they could be included in the control strategy, where the now constant values would simply be exchanged for measured values.

To simplify the equations above, we can gather the indoor temperatures of all buildings into one vector $\mathbf{T}$, and the dynamics can then be put on the following linear form:

$$\mathbf{T}(t_{k+1}) = A\mathbf{T}(t_k) + B_q\mathbf{q}(t_k) + B_{\text{ext}}T_{\text{ext}}(t_k) \tag{10}$$

REMARK 2
In this model we do not take domestic hot water use into account, much due to the difficulty of including a realistic model of this usage. In a typical scenario, the flow q_i through each building would consist of two parts, one for space heating and one for hot water usage.

3.3 Distribution Model

This part formulates the constraints on hot water flows in the distribution network, the first contribution of this article. This corresponds to the set $\mathcal{Q}$ of equation (1c). This work considers primarily a simple network architecture corresponding to a line of N units, as seen in Figure 2. A central pump circulates the water through the pipes, and each substation, with index i, has a control valve that it can use to regulate the water flow q_i through their substation locally. Associate with each pipe and valve

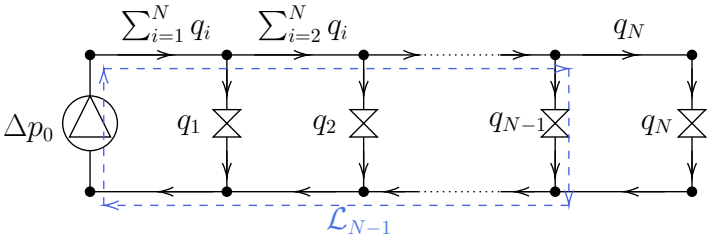

Figure 2. Simple network structure with only one heat source. Here equation (13) has already been used to calculate the flows in the supply and return pipes as a function of the substation flows q_i. Loop $N-1$ is illustrated with blue arrows.

a hydraulic resistance $a_i(t)$. $a_i(t)$ is constant for pipes and variable for valves, but bounded below by $a_i(t) \geq a_i^{\min}$ corresponding to a completely open valve. Note that the hydraulic resistance of supply pipes will be denoted $a_i^{\sup}$ and for return pipes a_i^{ret}.

The following equations dictate the relation between flows and pressure head in the network. For a pipe or valve i,

$$\Delta p_i = a_i(t) q_i^2, \tag{11}$$

where Δp_i is the pressure difference between the entrance and exit points of the component, caused by pressure losses due to friction [Frederiksen and Werner, 2013], [Wang et al., 2017]. For a pump j,

$$\Delta p_j = c_{1,j} q_j^2 + c_{2,j} r_j(t) + c_{3,j} r_j(t)^2 \tag{12}$$

where $c_{1,j}$, $c_{2,j}$ and $c_{3,j}$ are pump parameters that denote the characteristics of a specific pump, and $r_j(t) \leq 1$ is the pump frequency ratio indicating the capacity at which the pump is operating at.

Two laws apply to the flows and pressures in the network [Wang et al., 2017]:

1. The sum of directed flows entering a node is 0, so that the volume of water in a specific node does not change.
2. Traversing a loop of pipes in the network results in a zero net change in pressure.

1) can be expressed as

$$F\mathbf{q}(t) = 0, \tag{13}$$

where F is the incidence matrix of the network. The incidence matrix defines how all the pipes in the grid are connected to nodes (connection points) in the network and is defined as

$$F_{ij} = \begin{cases} 1, & \text{pipe j leads to node i} \\ -1, & \text{pipe j leads away from node i} \\ 0, & \text{pipe j is not connected to node i} \end{cases} \tag{14}$$

When applied to the network in Figure 2, we see that the flows in the supply-and-return pipes can be expressed as sums of the substation flows q_i. The second constraint 2) can be expressed as

$$\sum_{i \in \mathcal{L}_l} \Delta p_i = 0, \tag{15}$$

where $\mathcal{L}_l$ denotes the lth loop in the network, and Δp_i is the pressure difference along each edge that constitutes that loop [Sulzer Pumps, 2010], [Wang et al., 2017]. In Figure 2 we can identify N loops. Loop l starts in the central pump, goes through the supply pipes with resistances a_i^{sup}, then through the valve of substation l with resistance $a_l(t)$, and then back through the return pipes with resistances a_i^{ret}. The net pressure difference along this loop is then

$$\begin{aligned} &q_l(t)^2 a_l(t) + \sum_{j=1}^{l} \left(a_j^{\text{sup}} + a_j^{\text{ret}}\right) \left(\sum_{i=j}^{N} q_i(t)\right)^2 \\ &= c_1 \left(\sum_{i=1}^{N} q_i(t)\right)^2 + c_2 r(t) + c_3 r(t)^2, \end{aligned} \tag{16}$$

where the left expression is the pressure losses in the pipes and the right expression is the pressure head generated by the pump. There are N constraints on this form, one for each loop l for $l = 1 \ldots N$. Any flow q that satisfies the inequality

$$\begin{aligned} &q_l(t)^2 a_l^{\min} + \sum_{j=1}^{l} \left(a_j^{\text{sup}} + a_j^{\text{ret}}\right) \left(\sum_{i=j}^{N} q_i(t)\right)^2 \\ &\leq c_1 \left(\sum_{i=1}^{N} q_i(t)\right)^2 + c_2 + c_3 \end{aligned} \tag{17}$$

can also be made to satisfy the equation (16), by choosing a significantly large $r(t)$ and a sufficiently large $a_l(t)$. Therefore any flow that satisfies (17) can be actuated with sufficiently high pumping power and local regulation of the valves and any flow $\mathbf{q}$ that satisfies all of the N equations on the form (17) is feasible, i.e. $\mathbf{q} \in \mathcal{Q}$. Note that the equation (17) is convex in $\mathbf{q}$ (assuming c_1 negative). Therefore the set $\mathcal{Q}$, as the union of N convex sets on the form (17) and the constraints $\mathbf{q} \geq 0$, is also convex.

$$\mathcal{Q} = \{\mathbf{q} \,|\, \mathbf{q} \geq 0, \mathbf{q}^T M_l \mathbf{q} - c_2 - c_3 \leq 0, l = 1 \ldots N\} \tag{18}$$

$$M_l = D^T A D + E_{l,l} a_l^{\min} \tag{19}$$

Here D is an N by N upper triangular matrix of ones. A is an N by N diagonal matrix with entries $A_{1,1} = a_1^{\text{sup}} + a_1^{\text{ret}} - c_1$, $A_{i,i} = a_j^{\text{sup}} + a_j^{\text{ret}}$ for $2 \leq i \leq l$ and 0 otherwise. $E_{l,l}$ is an N by N matrix of all zeros, except for the element l,l, which is a one. This formulation makes M_l an N by N positive semidefinite matrix since A and $E_{l,l}$ have only positive diagonal entries, and thus $\mathcal{Q}$ is a union of quadratic and linear constraints, making it a convex set.

REMARK 3
The convexity of the set $\mathcal{Q}$ is connected to this specific grid structure, as the direction of the flow in this network is obvious. Indeed a meshed network is not guaranteed to enjoy this convexity of $\mathcal{Q}$, making optimization over the constraints on $\mathbf{q}$ harder to handle.

REMARK 4
Further operational constraints could also be introduced to restrict $\mathbf{q}$. For instance, too large flows may cause damage to pipes, or generate noise. An upper flow limitation could easily be added.

4. Control Strategies

This section investigates two potential control strategies, the *traditional* strategy and the *load coordination* strategy. An *optimal* baseline comparison is also introduced. The traditional architecture is where units are not connected through any sort of IT communication, and are simply attempting to maintain their own indoor temperature. In the load coordination architecture, the units calculate their desired loads locally through the exact same method as the traditional architecture, but these loads are then processed in a central computation and altered if they are not feasible. The optimal baseline is an upper bound on performance given the cost defined for the system. In this baseline it is assumed that a central unit has access to a perfect model of the entire system, as well as a posteriori measurements of the disturbance.

REMARK 5
Night set-back is an additional part of control strategies common in for instance Southern Europe. [Frederiksen and Werner, 2013] However, this work considers primarily the Northern European situation where this practice is less common and therefore it will not be considered.

4.1 Traditional Architecture

In traditional DH systems there is no IT communication between units in the network. Each unit will greedily evaluate their own desired flow q_i and actuate it

through their control valve. The central pump then ensures that the pressure difference between supply and return pipes in the network is high enough to allow these control valves to actuate any desired flow. Traditionally, the control for each individual building has been done through the following control loop: A temperature curve is calibrated for the building, where a reference temperature $T^{\mathrm{r}}_{\mathrm{hs},i}$ is set for the water circulating in the heating system, $T_{\mathrm{hs},i}$. A controller then tracks this reference through the control signal q_i, i.e. the flow through the substation heat exchanger primary side. This is actuated through altering the control valve opening $a_i(t)$. In this work we assume a simple proportional controller with gain k_i

$$T^{\mathrm{r}}_{\mathrm{hs},i} = \alpha_{0,i} + \alpha_{1,i} T_{\mathrm{ext}} \tag{20}$$

$$\tilde{q}_i = k_i (T^{\mathrm{r}}_{\mathrm{hs},i} - T_{\mathrm{hs},i}) \tag{21}$$

Here $\alpha_{0,i}$ and $\alpha_{1,i}$ are calibration parameters for the temperature curve. $\tilde{q}_i$ is the desired flow. When the distribution system is at maximum capacity, the differential pressure at unit i may be too low, and in that case the actual flow q_i will be lower than $\tilde{q}_i$. The tuning of the parameters would be done by hand by a technician, based on experience and knowledge of suitable parameters for similar buildings. When a unit is not constrained in the flow $q_i(t)$, the unit should be able to reject the influence of outdoor temperatures such that a stationary outdoor temperature should not cause a stationary deviation in indoor temperature. When investigating the model of each building (7), (8) and (21), we can find that this is fulfilled when

$$1 + R_{\mathrm{hs},i}\beta_i k_i + R_{\mathrm{ext},i}\beta_i k_i \alpha_{1,i} = 0, \tag{22}$$

$$\frac{1}{1-\alpha_{1,i}}\alpha_{0,i} = T_{c,i}. \tag{23}$$

The details of these relations are covered in Appendix 1. Parameters chosen in this way yield that the building will be able to reject the influence of outdoor temperature and maintain indoor temperature at comfort level. For simulation purposes, the parameters were chosen as

$$k_i = \frac{T_c}{\alpha_{0,i} R_{\mathrm{ext},i} - T_{c,i} R_{\mathrm{hs},i} - T_{c,i} R_{\mathrm{ext},i}} \tag{24}$$

$$\alpha_{1,i} = -\frac{1 + k_i R_{\mathrm{hs},i}}{k_i R_{\mathrm{ext},i}}. \tag{25}$$

$\alpha_{0,i}$ is simply chosen large enough that the denominator of (24) does not become negative.

REMARK 6

In practice, the actuator in the building substation is the control valve, and current implementations of control systems may use this actuator directly to control the

secondary side heating system temperature. In this case, the flow q becomes an output of the system rather than an input. This problem is readily overcome through standard cascade control. In this setup, the flow q will be the input that dictates the temperature of heating system water. This flow level will be the set-point for a secondary control loop where the valve position is used to actuate the desired flow. This adds the complexity of including the measurement of the flow into the control process. [Skogestad and Postlethwaite, 2005]

4.2 Load Coordination Architecture

The main contribution of this work is the proposition of the following control strategy: Each unit calculates their desired flow $\tilde{q}_i$ as per the traditional strategy of section 4.1, equations (20) and (21). However, a central device ensures feasibility and fairness by providing each unit with an adjustment δ_i so that the actuated flow will be $q_i = \tilde{q}_i + \delta_i$. In terms of IT communication and computational complexity, this method would be found between the traditional architecture and other optimization-based approaches. Depending on how δ_i is calculated, the central unit does not need access to internal building measurements, only their desired flow $\tilde{q}_i$. The explicit models of building dynamics i.e. equations (7) and (8) are not needed in the central computation. Instead only the tuning parameters of the controllers can be utilized. The tuning for the controllers in each building can be done in a distributed fashion, so that a technician working on one individual unit does not affect the control of the whole system.

The aim of the coordination is that the temperature deviations in each building should be distributed more fairly than in the non-coordinated traditional case. In Appendix 1, we show that given

- the models of the buildings presented in section 3.2, equations (7), (8) and (21)
- and the local unit controllers from section 4.1, equations (22) and (23),

then given a constant temperature disturbance, each unit will converge to the following stationary indoor temperature deviation from comfort e_i:

$$e_i = \frac{1}{k_i(1-\alpha_{1,i})}\delta_i \tag{26}$$

While this stationary deviation fails to capture the time dynamics of the system, it is still a valuable metric. Should the system be subject to a constant outdoor temperature lower than the system is able to reject due to flow constraints, then the indoor temperature deviations will align with this distribution. This motivates the following coordination strategy:

Define the parameters γ_i:

$$\gamma_i = \frac{1}{k_i(1-\alpha_{1,i})} \tag{27}$$

The interpretation of this parameter is a weight provided to each building, indicating how much the deviation δ_i will affect them. Units with large controller gain parameters (k_i and $\alpha_{1,i}$) will not be as impacted by the deviation term. The coordination then wants to minimize the weighted indoor temperature deviations, which can be formulated as the following optimization problem:

$$\underset{\delta}{\text{minimize}} \qquad \max_i |\lambda_i \gamma_i \delta_i| \tag{28}$$

$$\text{subject to} \qquad \tilde{\mathbf{q}} - \delta \in \mathcal{Q} \tag{29}$$

$\mathcal{Q}$ is a union of quadratic constraints, and the objective function can be reformulated as a linear program. Therefore this becomes a quadratic program where the number of constraints and decision variables grows linearly with the number of connected units, making the problem readily solvable by standard quadratic program solvers. The actual cost to minimize is J_∞ (6). This is a simplified problem where instead the central coordinator minimizes the weighted stationary temperature that would arise from the coordination terms δ_i. The weights λ_i are design parameters that could be used to capture the quality of service requirements of specific units. For instance a hospital with harsh climate requirements may have a larger λ_i than for example a residential building. In this work the influence of λ_i will not be investigated, and thus we will from now on assume $\lambda_i = 1$.

REMARK 7
Note that according to the current assumptions of individual unit controllers, this central coordination can be designed without explicit knowledge of the building parameters $R_{ext,i}$, $R_{hs,i}$, $C_{in,i}$ or $C_{hs,i}$. The modelling effort is left to each individual unit in the form of controller tuning.

4.3 Optimal Baseline

While we are interested in comparing the load coordination strategy to the traditional strategy, it is also interesting to see what the upper limit of optimality is. We consider the following problem

$$\min_{\mathbf{q}(t_k)} \qquad \sum_{k=0}^{K} \max_i \left(|e_i(t_k)t_s|\right) \tag{30a}$$

$$\text{subject to} \qquad \mathbf{T}(t_{k+1}) = A\mathbf{T}(t_k) + B_q\mathbf{q}(t_k) + B_{\text{ext}}T_{\text{ext}}(t_k), \tag{30b}$$

$$\mathbf{q}(t_k) \in \mathcal{Q}. \tag{30c}$$

$$\mathbf{T}(t_0) = \mathbf{T}_0. \tag{30d}$$

which can directly be solved by optimization solvers, as the problem is convex. The problem implies minimizing the cost J_∞ of equation (6), subject to the dynamical constraints of the system. For larger networks and longer time-horizons, it will no longer be feasible to solve the entire problem at once as we have done here without adding computational power.

It should be clarified that this optimal baseline as explored in this paper is only presented as a point of reference for comparison with the other methods. In reality it would be completely unfeasible to have exact knowledge of all system parameters, system states, and knowledge of future disturbances. This comparison serves to give an indication about how much possible improvement a given strategy could theoretically have, given our current cost-evaluation.

REMARK 8
It should be noted that this is distinct from online optimization-and-prediction based strategies such as MPC. Such methods rely on online measurements and predictions of disturbances and state evolutions. The optimal strategy in this work is an a posteriori optimization given full knowledge of disturbances and system models.

5. Simulation and Results

The first part of this section details the setup for the simulation experiments, followed by a part detailing the results.

5.1 Simulation Description

This work was simulated in Matlab, with optimization performed using Yalmip [Löfberg, 2004] with a Mosek optimizer. A network of $N = 25$ buildings, consisting of state space models as per section 3.2 was generated randomly. Controller parameters k_i, $\alpha_{0,i}$ and $\alpha_{1,i}$ were generated for each building in accordance with section 4.1. Random parameters were generated for pipes connecting these buildings in a line as per Figure 2, as well as parameters that describe the limits of customer substations. The random generation of parameters was done by setting a nominal value for parameters based on parameters from similar models in other works, and then uniformly generating the parameters in a range from these nominal values. The resulting parameters are listed in Table 2

The distribution pump curve (12) was generated the following way: The pump is dimensioned to handle a peak load that occurs at -15°C outdoor temperature. For each building connected to the grid, the flow required to keep the unit at comfort temperature given an outdoor temperature of -15°C, denoted $\mathbf{q}_i^{\text{peak}}$ was calculated, given equations (7) and (8). Using these flows in the left side of (16) with $a_l(t) =$

Table 2. Model parameters used for simulation.

Index	a^{ret}	a^{sup}	a^{min}	R_{hs}	R_{ext}	C_{hs}	C_{in}	T_c	α_0	α_1	k
Unit	mPa/(kg/s)^2	mPa/(kg/s)^2	mPa/(kg/s)^2	°C/kW	°C/kW	kJ/°C	kJ/°C	°C	°C	-	kg/s°C
1	8.22	8.22	160	275	272	22.6	1110	20	48.2	-1.41	9.15
2	3.14	3.14	64.7	281	301	22.4	1020	20	46.4	-1.32	8.59
3	5.18	5.18	286	225	299	18.9	1050	20	42.1	-1.1	9.54
4	4.28	4.28	297	282	264	21.6	1270	20	49.6	-1.48	9.17
5	7.78	7.78	179	262	261	16.7	1180	20	48.1	-1.4	9.58
6	5.39	5.39	179	223	288	22.1	1110	20	42.6	-1.13	9.79
7	8.49	8.49	139	236	321	15.3	1400	20	41.6	-1.08	8.97
8	3.77	3.77	285	255	277	17.8	1250	20	46.2	-1.31	9.4
9	4.3	4.3	148	285	294	15.5	1230	20	47.2	-1.36	8.63
10	3.54	3.54	80.7	285	268	16	1450	20	49.6	-1.48	9.03
11	3.47	3.47	254	227	306	23.2	1070	20	41.8	-1.09	9.37
12	8.23	8.23	153	286	270	21.9	1350	20	49.4	-1.47	8.99
13	6.35	6.35	114	285	288	18.2	1350	20	47.7	-1.39	8.72
14	6.16	6.16	157	251	302	24.5	1130	20	43.9	-1.2	9.04
15	3.53	3.53	76.8	274	316	15.3	1240	20	44.8	-1.24	8.48
16	8.12	8.12	86	226	321	19.4	946	20	40.9	-1.05	9.14
17	6.62	6.62	296	246	291	18.8	932	20	44.3	-1.21	9.3
18	4.87	4.87	300	282	262	22.7	1220	20	49.8	-1.49	9.19
19	5.92	5.92	201	273	263	23	1370	20	48.9	-1.45	9.33
20	5.2	5.2	67.3	285	271	16.9	1460	20	49.3	-1.46	9
21	3.08	3.08	113	263	313	19.9	978	20	44.2	-1.21	8.68
22	4.15	4.15	143	219	270	19.5	1240	20	43.4	-1.17	10.2
23	3.39	3.39	265	277	311	21.5	1180	20	45.4	-1.27	8.51
24	3.78	3.78	55.8	283	270	22.1	907	20	49.2	-1.46	9.05
25	4.15	4.15	63	265	319	22.5	1100	20	43.9	-1.2	8.56

$a_l^{\max}$, the pressure generated by the pump p^{peak} can be calculated.

$$p^{\text{peak}} = \max_l \left(q_l^{\text{peak}\ 2} a_l^{\min} + \sum_{j=1}^{l} \left(a_j^{\sup} + a_j^{\text{ret}} \right) \left(\sum_{i=j}^{N} q_i^{\text{peak}} \right)^2 \right) \tag{31}$$

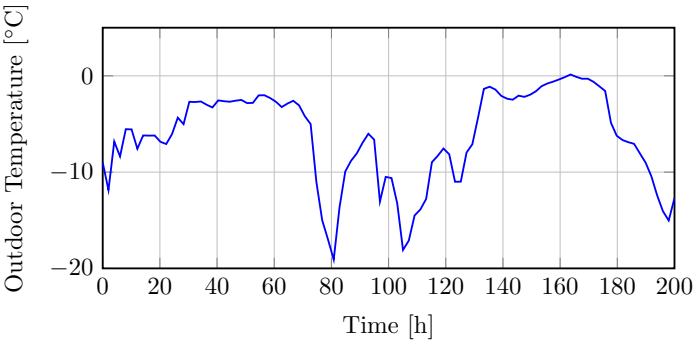

Figure 3. Outdoor temperature curve used for simulation.

It is then assumed that at this peak flow rate, the pump is running at full capacity, $r(t) = 1$. The parameters c_i are then found by solving the equation

$$c_1 \left(\sum_{i=1}^{N} q_i^{\text{peak}} \right)^2 + c_2 + c_3 = p^{\text{peak}} \tag{32}$$

such that c_i are proportional to the corresponding parameters in other literature [Wang et al., 2017].

The system was then simulated subject to an outdoor temperature curve generated from real data. The data was gathered from [Swedish Meteorological & Hydrological Institute, n.d.], from a region in Sweden, chosen to represent a time period of drastically dropping temperature. The readings are hourly measurements and were therefore linearly interpolated to 15 minute intervals in the simulation. The resulting temperature curve is visible in Figure 3. The simulation was done for each of the above listed architectures.

5.2 Results

Figures 4a, 4b and 4c show the evolution of indoor temperatures using the traditional strategy, load coordination strategy and optimal baseline respectively. Recall from the problem formulation of section 3.1 that no unit should experience heavy temperature deviations from the comfort temperature of 20°C. The clear distinction between the strategies is that using the traditional architecture results in a few units deviating greatly from their desired indoor temperature. Using the load coordination strategy, the units are much more aligned, leading to all units experiencing deviations but on a much lower magnitude. Finally, in the optimal baseline the results are even better. The units hardly deviate at all from their desired temperatures, and temperatures are deviating equally between all units. In this baseline the units are also pre-heated before the severe drop in temperature, which is not incorporated in

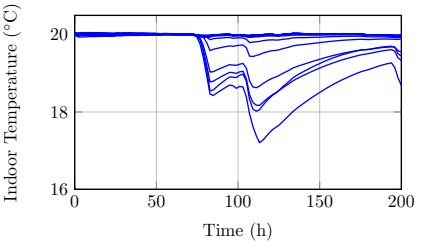

(a) Indoor temperature, traditional strategy.

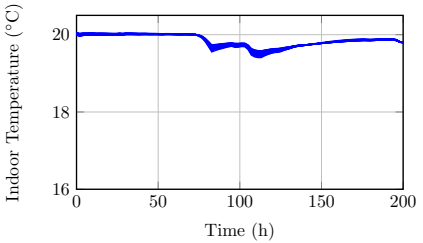

(b) Indoor temperature, load coordination strategy.

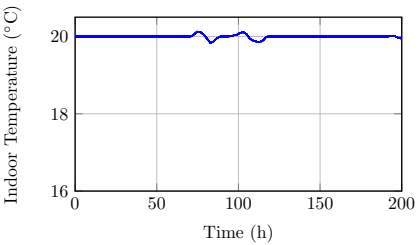

(c) Indoor temperature, optimal baseline.

Figure 4. Indoor temperatures registered during the simulation.

the other strategies as they do not include any predictive behaviour.

The plots of Figures 4 give a hint of what the effect of the different strategies are. However they are also supported by Figure 5. Here the discomfort metric of equation (3) are shown, evaluated on each strategy and unit. Figure 5a shows the inequality generated by the traditional strategy, as units located further from the heat source experience higher discomfort. Meanwhile, Figure 5b shows a much more equal distribution of discomfort. Lastly, Figure 5c shows that there is still a discrepancy between the coordinated strategy and the theoretical lower bound on discomfort.

Figure 6 shows the different discomfort metrics of (4), (5) and (6) evaluated through each coordination strategy, corresponding to J_1, J_2 and J_∞ respectively. We see that the sum of discomfort experienced in units, corresponding to J_1, is actually improved using traditional architecture than the load coordination architecture. This is quite reasonable, since providing higher flow to units further down the network incurs a higher pressure loss. Thus the total flow provided in the traditional strategy is higher. However, when measured through J_2 and J_∞, the load coordination strategy outperforms the traditional strategy. This is because the worst-case experience for any unit is much lower with this setup. The optimal baseline shows that there is still potential improvements to be made.

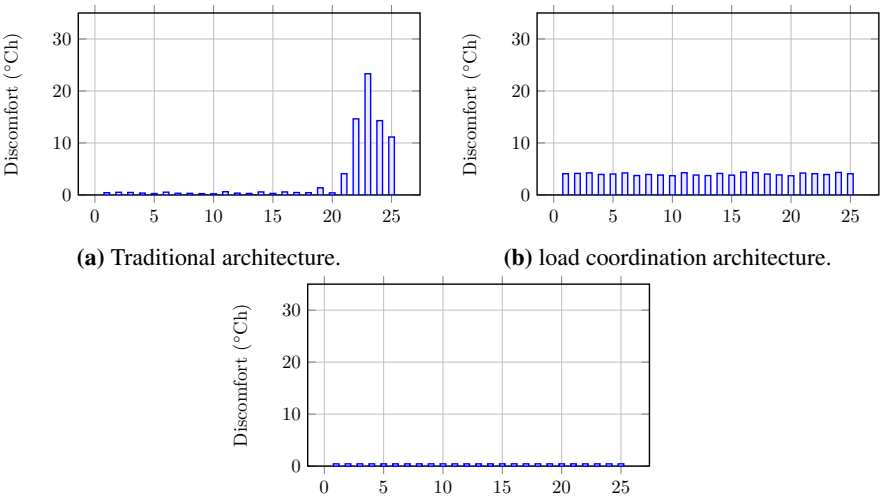

(a) Traditional architecture.

(b) load coordination architecture.

(c) Optimal baseline.

Figure 5. Discomfort experienced by each individual building, indexed 1-25 by their distance from the central distribution pump where 25 is the furthest.

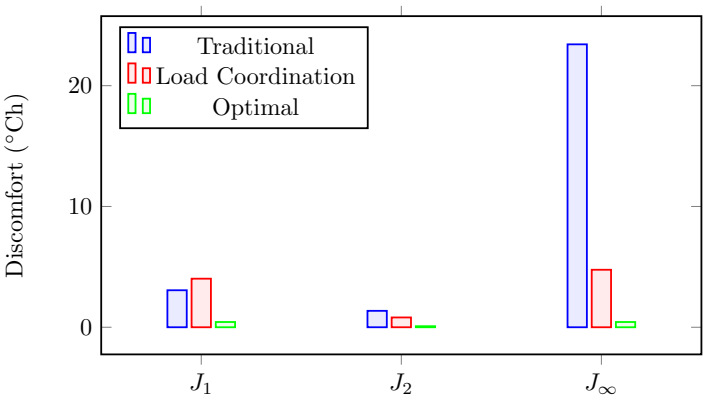

Figure 6. Discomfort metrics defined in equations (4), (5) and (6) (J_1, J_2 and J_∞ respectively) evaluated through each coordination strategy.

6. Summary

This section concludes the work with some final remarks, followed by potential future outlooks.

6.1 Conclusions

In this work, we investigated the influence of two different architectures for coordinating the flows in a line-structured district heating network. It was shown that utilizing traditional control strategies in each unit can be augmented with a coordination mechanism which reduces the worst-case discomfort experienced by any unit under peak load conditions, at the cost of increasing the mean discomfort, see Figure 6. This coordination can be achieved without explicit models or temperature readings accessed by the central unit. This proof of concept shows how augmenting future district heating systems with smarter controllers can increase the systems' robustness to peak load conditions. The design requirements for future district heating grids can therefore be lowered, allowing for lower grid temperature without as much additional grid capacity in terms of extended piping and pumping power.

However, further improvements can be made to the control strategy when utilizing an optimization-based architecture that allows utilizing information on temperature forecasts to pre-heat units ahead of peak loads. This requires even further complexity, where the central computation unit would have access to individual unit measurements, unit building parameters, and accurate weather forecasts.

The fact that the coordination strategy does not rely on building temperature measurements, and that controllers can be tuned individually for units without affecting the tuning of other units, makes the strategy scalable to growing networks as well as a more privacy-compliant option than a full optimization-based scheme.

6.2 Future Work

The proposed coordination strategy currently does not include the intelligent behavior of the optimal baseline, where the unit indoor temperatures can be utilized for pre-heating before load peaks, often referred to as peak-shaving and valley-filling. The main interest here would be to see if the architecture could maintain the autonomy of unit controllers, while simultaneously including predictive behavior based on an outdoor temperature forecast.

Both the optimal strategy and the proposed coordination strategy currently rely on understanding the set $\mathcal{Q}$ that describes the set of possible flows. This may in practice be harder estimate than proposed in this work, as specific and accurate parameters for all network parameters may not be known, or degrade and change over time. Therefore it would be interesting to see how these methods hold to uncertainties in network models, as well as data driven methods for estimating the parameters that dictate $\mathcal{Q}$. While the building model parameters are technically not necessary in the controller coordination, it is reasonable to believe that building controllers will not be as perfectly tuned as proposed in this work. Therefore a study should be conducted to investigate the sensitivity to poorly tuned individual

building controllers.

To further simplify the tuning of individual unit controllers, it is likely that more sophisticated unit controllers should be utilized. For instance, a simple PI-controller would allow the elimination of stationary errors when tracking the reference heating system temperature. Therefore including more advanced individual controllers in the analysis would be a valuable extension.

7. Acknowledgements

This work is funded by the European Research Council (ERC) under the European Union's Horizon 2020 research and innovation program under grant agreement No 834142 (ScalableControl).

APPENDIX A - Individual Unit Controller Tuning

This appendix presents the motivating equations behind the tuning of traditional unit controllers and the choice of weights γ_i used in the load coordinating architecture.

To investigate the effects of the control parameters k_i, $\alpha_{0,i}$, $\alpha_{1,i}$ as well as the coordination signal δ_i, we combine equations (7), (8), (9) and (21). This grants the following system description of the unit:

$$\begin{pmatrix} \dot{T}_{\text{in},i} \\ \dot{T}_{\text{hs},i} \end{pmatrix} = A \begin{pmatrix} T_{\text{in},i} \\ T_{\text{hs},i} \end{pmatrix} + B \begin{pmatrix} T_{\text{ext}} \\ \delta_i \end{pmatrix} + C \tag{A.1}$$

where

$$A = \begin{pmatrix} -\frac{1}{R_{\text{ext},i}} - \frac{1}{R_{\text{hs},i}} & \frac{1}{R_{\text{hs},i}} \\ \frac{1}{R_{\text{hs},i}} & -\frac{1}{R_{\text{hs},i}} - C_w(T_{\text{sup}} - T_{\text{ret}})k_i \end{pmatrix} \tag{A.2}$$

$$B = \begin{pmatrix} \frac{1}{R_{\text{ext},i}} & 0 \\ C_w(T_{\text{sup}} - T_{\text{ret}})k_i\alpha_{1,i} & C_w(T_{\text{sup}} - T_{\text{ret}}) \end{pmatrix} \tag{A.3}$$

and

$$C = \begin{pmatrix} 0 \\ C_w(T_{\text{sup}} - T_{\text{ret}})k_i\alpha_{0,i} \end{pmatrix} \tag{A.4}$$

Note that these matrices A and B are not the same matrices as in equation (10). A feasible target for the design of the control parameters k_i, $\alpha_{0,i}$ and $\alpha_{1,i}$ is that when there is no coordination signal δ_i, the building should, given a constant outdoor temperature T^0_{ext}, be able to reach a given comfort temperature $T_{c,i}$ indoors. We therefore investigate the stationary case where $\dot{T}_{\text{in},i} = \dot{T}_{\text{hs},i} = 0$, $T_{\text{ext}} = T^0_{\text{ext}}$ and $\delta_i = \delta^0_i$. We can find the resulting indoor and heating system temperatures as

$$\begin{pmatrix} T^0_{\text{in},i} \\ T^0_{\text{hs},i} \end{pmatrix} = -A^{-1}B \begin{pmatrix} T^0_{\text{ext}} \\ \delta^0_i \end{pmatrix} - A^{-1}C. \tag{A.5}$$

Introducing $\beta_i = C_w(T_{\text{sup}} - T_{\text{ret}})$ for brevity, this yields the following stationary indoor temperature:

$$T^0_{\text{in},i} = \frac{1 + R_{\text{hs},i}\beta_i k_i + R_{\text{ext},i}\beta_i k_i \alpha_{1,i}}{1 + R_{\text{ext},i}\beta_i k_i + R_{\text{hs},i}\beta_i k_i} T^0_{\text{ext}} \tag{A.6}$$

$$+ \frac{R_{\text{ext},i}\beta_i}{1 + R_{\text{ext},i}\beta_i k_i + R_{\text{hs},i}\beta_i k_i} \delta^0 \tag{A.7}$$

$$+ \frac{R_{\text{ext},i}\beta_i k_i}{1 + R_{\text{ext},i}\beta_i k_i + R_{\text{hs},i}\beta_i k_i} \alpha_{0,i} \tag{A.8}$$

The temperature deviation caused by the external temperature is captured in the term (A.6). To ensure that the outdoor temperature does not cause systematic temperature deviations, the controller gains will have to be chosen so that

$$1 + R_{\text{hs},i}\beta_i k_i + R_{\text{ext},i}\beta_i k_i \alpha_{1,i} = 0 \tag{A.9}$$

Substituting equation (A.9) into the terms (A.6), (A.7) and (A.8), we receive the following resulting indoor temperature:

$$T^0_{\text{in},i} = \frac{1}{k_i(1 - \alpha_{1,i})} \delta^0 \tag{A.10}$$

$$+ \frac{1}{1 - \alpha_{1,i}} \alpha_{0,i} \tag{A.11}$$

From here, we see that a suitable choice of $\alpha_{0,i}$ is so that the relation

$$\frac{1}{1 - \alpha_{1,i}} \alpha_{0,i} = T_{c,i} \tag{A.12}$$

is fulfilled, i.e. given no coordination term δ_i, the unit should experience comfort temperature.

The remaining deviation caused by the coordination term δ_i is demonstrated in equation (A.10), motivating the weights chosen in section 4.2.

References

Bacher, P. and H. Madsen (2011). "Identifying suitable models for the heat dynamics of buildings". en. *Energy and Buildings* **43**:7, pp. 1511–1522. ISSN: 03787788. DOI: 10.1016/j.enbuild.2011.02.005. URL: https://linkinghub.elsevier.com/retrieve/pii/S0378778811000491 (visited on 2021-07-14).

Benonysson, A., B. Bøhm, and H. Ravn (1995). "Operational optimization in a district heating system". en. *Energy Conversion and Management* **36**, pp. 297–314.

Bhattacharya, S., C. V., A. V., and K. K. (2019). "Demand response for thermal fairness in district heating networks". en. *IEEE Transactions on Sustainable Energy* **10**:2, pp. 865–875. ISSN: 1949-3029, 1949-3037. DOI: 10.1109/TSTE.2018.2852629. URL: https://ieeexplore.ieee.org/document/8402142/ (visited on 2021-07-05).

Brange, L., K. Sernhed, and M. Thern (2019). "Decision-making process for addressing bottleneck problems in district heating networks". en. *International Journal of Sustainable Energy Planning and Management* **20**, pp. 37–50.

Frederiksen, S. and S. Werner (2013). *District heating and cooling*. Studentlitteratur. Chap. 2.

Guelpa, E. and V. Verda (2021). "Demand response and other demand side management techniques for district heating: A review". en. *Energy* **219**. ISSN: 03605442. DOI: 10.1016/j.energy.2020.119440. URL: https://linkinghub.elsevier.com/retrieve/pii/S0360544220325470.

Larsen, H., H. Pálsson, B. Bøhm, and H. Ravn (2002). "Aggregated dynamic simulation model of district heating networks". en. *Energy Conversion and Management* **43**:8, pp. 995–1019. ISSN: 01968904. DOI: 10.1016/S0196-8904(01)00093-0. URL: https://linkinghub.elsevier.com/retrieve/pii/S0196890401000930 (visited on 2021-08-20).

Löfberg, J. (2004). "Yalmip : a toolbox for modeling and optimization in matlab". In: *In Proceedings of the CACSD Conference*. Taipei, Taiwan.

Lund, H., S. Werner, R. Wiltshire, S. Svendsen, J. Thorsen, F. Hvelplund, and B. Mathiesen (2014). "4th generation district heating (4GDH)". *Energy* **68**, pp. 1–11. ISSN: 03605442. DOI: 10.1016/j.energy.2014.02.089. URL: https://linkinghub.elsevier.com/retrieve/pii/S0360544214002369 (visited on 2021-07-14).

Lund, H., P. A. Østergaard, M. Chang, S. Werner, S. Svendsen, P. Sorknæs, J. E. Thorsen, F. Hvelplund, B. O. G. Mortensen, B. V. Mathiesen, C. Bojesen, N. Duic, X. Zhang, and B. Möller (2018). "The status of 4th generation district heating: research and results". *Energy* **164**, pp. 147–159. ISSN: 0360-5442. DOI: https://doi.org/10.1016/j.energy.2018.08.206. URL: https://www.sciencedirect.com/science/article/pii/S0360544218317420.

Lund, R., D. østergaard, X. Yang, and B. Mathiesen (2017). "Comparison of low-temperature district heating concepts in a long-term energy system perspective". *International Journal of Sustainable Energy Planning and Management* **12**, pp. 5–18. DOI: https://doi.org/10.5278/ijsepm.2017.12.2.

Mathiesen, B., H. Lund, D. Connolly, H. Wenzel, P. Østergaard, B. Möller, S. Nielsen, I. Ridjan, P. Karnøe, K. Sperling, and F. Hvelplund (2015). "Smart energy systems for coherent 100% renewable energy and transport solutions". *Applied Energy* **145**, pp. 139–154. ISSN: 0306-2619. DOI: https://doi.org/10.1016/j.apenergy.2015.01.075. URL: https://www.sciencedirect.com/science/article/pii/S0306261915001117.

Saletti, C., A. Gambarotta, and M. Morini (2020). "Development, analysis and application of a predictive controller to a small-scale district heating system". en. *Applied Thermal Engineering* **165**. ISSN: 13594311. DOI: 10.1016/j.applthermaleng.2019.114558. URL: https://linkinghub.elsevier.com/retrieve/pii/S135943111935392X (visited on 2021-07-14).

Sarbu, I., M. Mirza, and E. Crasmareanu (2019). "A review of modelling and optimisation techniques for district heating systems". *International Journal of Energy Research*, pp. 6572–6598. ISSN: 0363-907X, 1099-114X. DOI: 10.1002/er.4600. URL: https://onlinelibrary.wiley.com/doi/10.1002/er.4600 (visited on 2021-07-14).

Skogestad, S. and I. Postlethwaite (2005). *Multivariable Feedback Control: Analysis and Design*. 2nd. John Wiley & Sons Ltd, Chichester, p. 423.

Sulzer Pumps (2010). *Centrifugal pump handbook*. Ed. by Sulzer Pumps. 3rd. Butterworth-Heinemann, Oxford, pp. 27–68. ISBN: 978-0-7506-8612-9. DOI: https://doi.org/10.1016/B978-0-7506-8612-9.00002-4. URL: https://www.sciencedirect.com/science/article/pii/B9780750686129000024.

Swedish Meteorological & Hydrological Institute (n.d.). https://www.smhi.se/en/services/open-data/search-smhi-s-open-data-1.81004.

Vandermeulen, A., B. van der Heijde, and L. Helsen (2018). "Controlling district heating and cooling networks to unlock flexibility: A review". en. *Energy* **151**, pp. 103–115. ISSN: 03605442. DOI: 10.1016/j.energy.2018.03.034. URL: https://linkinghub.elsevier.com/retrieve/pii/S0360544218304328 (visited on 2021-07-14).

Wang, Y., S. You, H. Zhang, W. Zheng, X. Zheng, and Q. Miao (2017). "Hydraulic performance optimization of meshed district heating network with multiple heat sources". *Energy* **126**, pp. 603–621. DOI: 10.1016/j.energy.2017.03.044.

Paper II

Hydraulic Parameter Estimation in District Heating Networks

Felix Agner Pauline Kergus Richard Pates Anders Rantzer

Abstract

Using hydraulic models in control design in district heating networks can increase pumping efficiency and reduce sensitivity to hydraulic bottlenecks. These models are usually white-box, as they are obtained based on full knowledge of the district heating network and its parameters. This type of model is time-consuming to obtain, and might differ from the actual behavior of the system. In this paper, a method is proposed to obtain a grey-box hydraulic model for tree-shaped district heating systems: hydraulic parameters are estimated based on pressure measurements in only two locations. While previous works only estimate parameters related to pressure losses in pipes, this work also includes customers valves in the grey-box model structure, an important inclusion for control-oriented applications. Finally, a numerical example illustrates the proposed method on a small district heating network, showing its ability to obtain an accurate model on the basis of noisy measurements.

Originally published at IFAC 2023, Yokohama. Reprinted with permission.

This work is funded by the European Research Council (ERC) under the European Union's Horizon 2020 research and innovation program under grant agreement No 834142 (ScalableControl).

1. Introduction

District heating networks already play an important role in the energy mix of some countries, such as Sweden and Denmark, see [Frederiksen and Werner, 2013]. As mentioned in [Lund et al., 2018], district heating (and cooling) has an important role to play in the transition to future sustainable energy solutions. As underlined in [Vandermeulen et al., 2018], it is required to tackle several control challenges to utilize the full potential of district heating in these future systems. In particular, [Vandermeulen et al., 2018] recalls that enabling low supply temperatures and ensuring a fair distribution of heat (and cold) is important in the transition to more efficient district heating networks. Both aspects are linked to the regulation of flow rates. Indeed, lowering the supply temperature can lead to higher flow rates, which may create bottlenecks ([Brange et al., 2019]). Bottlenecks are events of insufficient differential pressure between supply and return pipes in some parts of the network, caused by significant pressure losses.

In this context, regulating the flow in district heating networks is an important control problem, not only in future generations of district heating but already in existing networks, see [Frederiksen and Werner, 2013]. In this flow control perspective, considering a hydraulic model of district heating networks can be beneficial. [Wang et al., 2017] showed that using such a model can reduce the necessary pumping power. [Agner et al., 2022] showed that hydraulic models can be used to reduce the effect of bottlenecks in times of peak demand.

Hydraulic modelling is usually white-box, see [Frederiksen and Werner, 2013]. Pressure losses in pipes are described using lengths, diameters and friction coefficients. Valves are modelled with characteristics provided by manufacturers. Such white-box models require gathering a lot of information, which may be complicated in practice. In addition, there is no guarantee that the model will fit the actual behavior of the district heating network. This paper aims at proposing a method to estimate a grey-box hydraulic model from measured data. Such data-driven modelling allows not only to save time in the modelling process, but also keeps the model accurate with regards to measurements.

Estimation of hydraulic model parameters has been investigated for water distribution systems, as summarized in [Savic et al., 2009]. However, only a few works have been published in the specific area of district heating systems, for which the models will differ in structure. [Yin et al., 2018] estimates a hydraulic model based on all nodal pressure head values in the network. [Wang et al., 2018] and [Liu et al., 2020] conducted similar studies, using measurements of pressures at all customer substations. Loop structured graphs are treated in [Liu et al., 2020] by working with

several overlapping tree-structured graphs. These works have shown that hydraulic parameter estimation from data is possible in theory. However, their identification process only accounts for pipes. Customer valves are neglected. Each such valve influences the pressure in the whole network and they are therefore important to consider for flow control purposes. This paper extends the work of [Liu et al., 2020] and [Wang et al., 2018] by introducing a parameterized valve model in the grey-box identification process. In addition, the assumption that nodal heads are measured at every substation is alleviated. This raises the question of whether all parameters in the network can still be uniquely identified.

The contributions of this work are as follows.

1. The non-linear hydraulic relations of a tree-structured district heating network are reduced to a set of equations which are linear with regards to the parameters under consideration.

2. The conditions for these equations to have a unique solution are provided, analyzed, and shown likely to hold in practice. This allows parameter estimation to be performed with a simple least square solution.

3. A numerical example demonstrates the feasibility of the method, based on noisy measurements.

Section 2 introduces the notation used to describe the considered networks, along with constraints related to flows and pressure in the network. The linear set of equations are presented in section 3. The conditions for a unique solution to the equations is analyzed in section 4. Finally the numerical example is presented in section 5.

2. Network Constraints

This section introduces notation for describing the considered networks, followed by models and constraints related to flows and pressures in the network.

2.1 Network Description

The type of network under consideration consists of two directed sub-graphs, a *supply-network* $\bar{\mathcal{G}} = (\bar{\mathcal{E}}, \bar{\mathcal{N}})$ and a *return-network* $\underline{\mathcal{G}} = (\underline{\mathcal{E}}, \underline{\mathcal{N}})$. They are symmetric in structure. In addition, there is a set of *boundary edges* $\mathring{\mathcal{E}}$ that are connected from some nodes in $\bar{\mathcal{N}}$ to their equivalent counterparts in $\underline{\mathcal{N}}$. Define also two reference nodes $\alpha \in \bar{\mathcal{N}}$ and $\beta \in \underline{\mathcal{N}}$, and assume all edges in $\bar{\mathcal{E}}$ and $\underline{\mathcal{E}}$ to be directed away from α and β respectively. Non-reference nodes which are not connected to a boundary edge are called *internal nodes*, and are assumed to have at least degree three. Denote a path $\mathcal{P}$ to be a set of ordered edges traversing a set of ordered, distinct nodes.

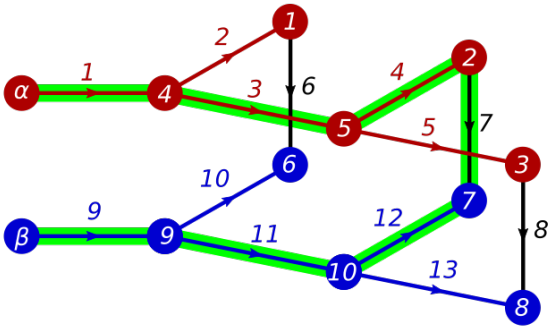

Figure 1. Small example network illustrating the network structure. Red edges and nodes are part of the supply-network, blue edges and nodes are part of the return network, and the black edges are the boundary edges. The green highlight shows a path $\mathcal{P}$.

Figure 1 illustrates such a network. Here $\bar{\mathcal{N}} = (\alpha, 1, 2, 3, 4, 5)$, $\underline{\mathcal{N}} = (\beta, 6, 7, 8, 9, 10)$, $\bar{\mathcal{E}} = (1, 2, 3, 4, 5)$ $\underline{\mathcal{E}} = (9, 10, 11, 12, 13)$ and $\mathring{\mathcal{E}} = (6, 7, 8)$. Internal nodes are 4, 5, 9 and 10. The highlighted path $\mathcal{P} = (1, 3, 4, 7, 12, 11, 9)$ traverses the nodes $(\alpha, 4, 5, 2, 7, 10, 9, \beta)$.

Associate each edge e with a volumetric flow rate q_e. Denote the vectors of such flows $\bar{q}$, $\underline{q}$ and $\mathring{q}$ for supply, return and boundary edges respectively. Associate with each node n a pressure-value p_n. Denote the vectors of such pressures $\bar{p}$ and $\underline{p}$ for supply and return nodes respectively. Associate with each edge e a control value $u_e \in]0, 1]$, and let $u_e = 1$ for $e \in \bar{\mathcal{E}} \cup \underline{\mathcal{E}}$. An edge e also has an unknown resistance parameter s_e, which is the parameter we seek to estimate in this paper. Denote $\bar{s}$, $\underline{s}$ and $\mathring{s}$ to be the vectors of such parameters related to edges in $\bar{\mathcal{E}}$, $\underline{\mathcal{E}}$ and $\mathring{\mathcal{E}}$ respectively. Assume symmetry between characteristics of supply and return edges such that $\bar{s} = \underline{s}$.

2.2 Flow model

Each node is subject to preservation of mass, i.e. the sum of incoming flow must equal the sum of outgoing flow. Considering first the supply-network, this can be equivalently written as

$$\begin{bmatrix} \mathring{q} \\ 0 \end{bmatrix} = \bar{B}\bar{q} \tag{1}$$

where $\bar{B} = [\bar{B}_{i,j}]$ is the basic incidence matrix of $\bar{\mathcal{G}}$, defined as

$$\bar{B}_{i,j} = \begin{cases} 1, & \text{if edge j leads to node i} \\ -1, & \text{if edge j leads away from node i} \\ 0, & \text{if edge j is not connected to node i.} \end{cases} \tag{2}$$

Here the node α is omitted to ensure (1) is not over-determined. Note that in (1), it is assumed without loss of generality that the nodes are ordered such that internal

nodes come last. See e.g. the network visible in Figure 1 for which

$$\bar{B} = \begin{bmatrix} 0 & 1 & 0 & 0 & 0 \\ 0 & 0 & 0 & 1 & 0 \\ 0 & 0 & 0 & 0 & 1 \\ 1 & -1 & -1 & 0 & 0 \\ 0 & 0 & 1 & -1 & -1 \end{bmatrix}. \tag{3}$$

Due to the tree-structure of $\bar{\mathcal{G}}$, $\bar{B}$ is invertible. This means that given known boundary flows $\mathring{q}$, the supply-flows $\bar{q}$ can be calculated as

$$\bar{q} = \bar{B}^{-1} \begin{bmatrix} \mathring{q} \\ 0 \end{bmatrix}. \tag{4}$$

Due to symmetry between $\bar{\mathcal{G}}$ and $\underline{\mathcal{G}}$, the corresponding basic incidence matrix $\underline{B} = \bar{B}$. This in combination with the boundary flows $\mathring{q}$ being directed from $\bar{\mathcal{G}}$ to $\underline{\mathcal{G}}$ gives

$$\underline{q} = -\bar{q}. \tag{5}$$

2.3 Differential pressure model

For an edge e with flow q_e, directed from node n to node m with pressures p_n and p_m, models of the following type are considered.

$$p_n - p_m = f(q_e, u_e)s_e, \tag{6}$$

where s_e is the unknown resistance parameter to estimate and $f : \mathbb{R} \times]0,1] \to \mathbb{R}$ is a given continuous function satisfying

$$f(q,u) = -f(-q,u), \tag{7}$$
$$f(0,u) = 0, \tag{8}$$
$$q_i > q_j \implies f(q_i,u) > f(q_j,u), \tag{9}$$
$$u_i > u_j \implies f(q,u_i) < f(q,u_j), \tag{10}$$
$$q > 0 \implies \lim_{u \to 0} f(q,u) = \infty,. \tag{11}$$

A specific choice of f will be presented in section 5, where a numerical example is investigated.

Consider all paths $\mathcal{P}_v$ that lead from α to β via a boundary edge $v \in \mathring{\mathcal{E}}$. Denote n_b to be the number of such paths, i.e. the number of boundary edges. The path $\mathcal{P}$ in Figure 1 is an example of such a path. Then

$$p_\alpha - p_\beta = \sum_{e \in \mathcal{P}_v \cap \bar{\mathcal{E}}} f(q_e,1)s_e - \sum_{e \in \mathcal{P}_v \cap \underline{\mathcal{E}}} f(q_e,1)s_e + f(q_v,u_v)s_v \tag{12}$$

for all v. This equation is the result of subsequent uses of (6). Note that $e \notin \mathring{\mathcal{E}} \implies u_e = 1$. The signs in front of the sums are decided by the direction of edges in the supply (return) network being directed from α (β).

Since $\bar{\mathcal{G}}$ and $\underline{\mathcal{G}}$ are symmetrical, the sets $\mathcal{P}_v \cap \bar{\mathcal{E}}$ and $\mathcal{P}_v \cap \underline{\mathcal{E}}$ contain the symmetrically corresponding edges. Using (5), (7) and the assumption $\bar{s} = \underline{s}$,

$$p_\alpha - p_\beta = \sum_{e \in \mathcal{P}_v \cap \bar{\mathcal{E}}} 2f(q_e, 1)s_e + f(q_v, u_v)s_v. \tag{13}$$

Considering (13) for all n_b paths at once yields

$$Fs = \mathbf{1}(p_\alpha - p_\beta). \tag{14}$$

Here $s = \left[\bar{s}^T, \mathring{s}^T\right]^T$ is a vector of n_s resistances and $F = [F_{i,j}]$ is an $n_b \times n_s$ matrix defined as

$$F_{i,j} = \begin{cases} 2f(q_j, 1), & \text{if } j \in \mathcal{P}_i \cap \bar{\mathcal{E}} \\ f(q_j, u_j), & \text{if } j \in \mathcal{P}_i \cap \mathring{\mathcal{E}} \\ 0, & \text{else.} \end{cases} \tag{15}$$

3. Linear Constraints for Hydraulic Parameter Estimation

This section presents a set of equations which is linear in the parameters s, and presents a parameter estimation method based on these constraints.

3.1 The Parameter Estimation Problem

For parameter estimation, we will use several samples of steady state measurements. Denote any such steady state of pressures, flows and valve positions in the network a *load condition* t. For example $\mathring{q}(t)$ is the vector of boundary flows $\mathring{q}$ at load condition t. The parameter estimation problem is therefore:

PROBLEM 1
Given load conditions $t = 1 \dots T$ with measurements of pressures $p_\alpha(1) \dots p_\alpha(T)$ and $p_\beta(1) \dots p_\beta(T)$, controller settings $u(1), \dots, u(T)$ and boundary flows $\mathring{q}(1), \dots, \mathring{q}(T)$, find an estimate $\hat{s}$ of the resistances s, such that $\hat{s} = s$.

3.2 Linear constraints

Let $F(t)$ be defined by (14) for one load condition t. Note that $F(t)$ can be constructed using only the boundary flows $\mathring{q}(t)$ and the controller settings $u(t)$. Using the measurements defined in Problem 1, the equation

$$\begin{bmatrix} F(1) \\ F(2) \\ \vdots \\ F(T) \end{bmatrix} s = \begin{bmatrix} \mathbf{1}(p_\alpha(1) - p_\beta(1)) \\ \mathbf{1}(p_\alpha(2) - p_\beta(2)) \\ \vdots \\ \mathbf{1}(p_\alpha(T) - p_\beta(T)) \end{bmatrix} \tag{16}$$

can be constructed. Let Φ be the matrix in the left hand side of (16) and y be the right hand side of (16) such that (16) can be condensed to

$$\Phi s = y. \tag{17}$$

Note that linear constraints were constructed also in [Wang et al., 2018] and [Liu et al., 2020]. Our extension is twofold: They required the measurement of pressure at each boundary node, while we use only p_α and p_β. In addition we include modeling of the valve characteristics which is important for control applications.

3.3 Estimation method

If (17) has a unique solution, a solution $\hat{s}$ to problem 1 can be obtained as

$$\hat{s} = \Phi^\dagger y, \tag{18}$$

where † denotes the the Moore-Penrose pseudoinverse. In a real application, Φ and y will be subject to measurement noise as well as errors in the model assumption, and in this case (18) chooses the $\hat{s}$ of minimum Euclidean norm which minimizes the Euclidean distance between observed and estimated values for y. While (18) is the method used in this paper, the linear constraints of (17) can be used in other optimization frameworks. For instance, parameter positivity constraints, other cost functions or other parameter regularization methods could be considered.

4. Uniqueness of solution

Equation (18) solves problem 1 if the solution to (17) is unique. Showing that this is likely is the topic of this section.

4.1 Conditions for unique solution

THEOREM 1

Consider (17) *which is a compact form for* (16)*, and where each row of* (16) *is constructed through* (12) *for a given path $\mathcal{P}_v$ and load condition t. Then given load conditions $t = 1, \dots T$ and paths $\mathcal{P}_v$, from α to β through edge v for all $v \in \mathring{\mathcal{E}}$, the following statements are equivalent.*

i Equation (17) *has a unique solution*

ii $\nexists \lambda \in \mathbb{R}^{n_s}$, $\lambda \neq 0$, *such that* $\forall \mathcal{P}_v, \forall t$*:*

$$\sum_{e \in \mathcal{P}_v \cap \bar{\mathcal{E}}} 2f(q_e(t), 1)\lambda_e + f(q_v(t), u_v(t))\lambda_v = 0 \tag{19}$$

Proof. Equation (17) will have a unique solution if and only if Φ has no linearly dependent columns. Condition ii corresponds exactly to the equation

$$\Phi\lambda = 0, \tag{20}$$

i.e. Φ has a non-trivial right nullspace and thus linearly dependent columns. Since ii dictates that there is no such $\lambda \neq 0$, Φ must have no linearly dependent columns. □

Theorem 1 is stated in terms of each load condition t used in constructing Φ. However, if (19) does not hold in general, i.e. for any set of load conditions that could feasibly be sampled, it becomes unlikely to hold for all t if T is large. Thus Given general q_e, q_v, θ_v, we investigate if

$$\sum_{e \in \mathcal{P}_v \cap \bar{\mathcal{E}}} 2f(q_e, 1)\lambda_e + f(q_v, u_v)\lambda_v = 0 \tag{21}$$

holds for any $\lambda \neq 0$. If not, we can conclude that it's unlikely that (19) holds for all t unless load conditions were sampled with some form of bias.

4.2 Independence of Boundary Edge Pressure Drops

Assume that there is a $\lambda \neq 0$ such that (21) holds. In addition, assume there is a v such that $\lambda_v \neq 0$. That would imply that

$$f(q_v, u_v) = -\frac{\sum_{e \in \mathcal{P}_v \cap \bar{\mathcal{E}}} 2f(q_e, 1)\lambda_e}{\lambda_v}, \tag{22}$$

i.e. there is a function mapping flows q_e in edges in $\mathcal{P}_v$ to $f(q_v, u_v)$. As a contradiction, consider the following proposition.

PROPOSITION 1
Consider a given boundary flow $\mathring{q} > 0$, a corresponding $\bar{q}$ that satisfies (4) *and p_α, p_β such that*

$$f(q_v, 1)s_v \leq p_\alpha - p_\beta - \sum_{e \in \mathcal{P}_v \cap \bar{\mathcal{E}}} 2f(q_e, 1)s_e, \tag{23}$$

for all paths $\mathcal{P}_v$ from α to β via a boundary edge v. Then there exists control settings $0 < u \leq 1$ such that $\mathring{q}$, $\bar{q}$, u, p_α and p_β fulfill both flow constraints (1) *and pressure constraints* (6) *and is thus feasible. In addition, $f(q_v, u_v)$ fulfills*

$$f(q_v, u_v)s_v = p_\alpha - p_\beta - \sum_{e \in \mathcal{P}_v \cap \bar{\mathcal{E}}} 2f(q_e, 1)s_e. \tag{24}$$

for all v.

Proof. Since $\bar{q}$ was constructed from (4), $\bar{q}$ and $\mathring{q}$ (and thus also $\underline{q}$) must fulfill the flow constraints (1) of the system. In addition, since $u_e = 1$ and q_e is given for all edges e in the supply-and-return networks, the nodal pressures which solve (6) are known. Since f fulfills both (10) and (11), (23) is the condition for the existence of a feasible u_v such that (6) holds for each boundary edge. If the condition holds, then (24) corresponds to just that u_v. □

Proposition 1 shows that $f(q_v, u_v)$ is decided by (24), $f(q_v, u_v)$ is a sum of $p_\alpha - p_\beta$ and a function of the flows along the edges of the path. Since Proposition 1 states that any boundary flow vector $\mathring{q} > 0$ and sufficiently large $p_\alpha - p_\beta$ is feasible, $f(q_v, u_v)$ is clearly not only a function of the flows, but also $p_\alpha - p_\beta$. This contradicts (22). Thus if there is a λ that fulfills (21), then $\lambda_v = 0$.

4.3 Independence of Pressure Drops Along Paths

If $\lambda_v = 0$ as previously shown, then returning to (21) and analyzing one edge $i \in \mathcal{P}_v$ yields

$$f(q_i, 1) = \frac{\sum_{e \in \mathcal{P}_v \cap \bar{\mathcal{E}}, e \neq i} 2 f(q_e, 1) \lambda_e}{\lambda_i}. \tag{25}$$

I.e. there is a function of the other flows q_e in $\mathcal{P}_v$ yielding $f(q_i, 1)$. (9) gives that f is monotone in q_i. This means that (25) implies that q_i can be decided as a function of the other flows q_e in the path. To contradict this, consider the following proposition.

PROPOSITION 2
Consider $\tilde{\mathcal{P}} = (e_1, e_2, \ldots, e_p)$ to be a path along the supply network from α to a node $\gamma \in \bar{\mathcal{N}}$, where e_1 is the first edge of $\tilde{\mathcal{P}}$. Let $q_1, q_2, \ldots, q_p$ be the flows through these edges. Consider edge $i \in \tilde{\mathcal{P}}$ with flow q_i. Then given flows $q_1, \ldots q_{i-1}$ and $q_i + 1 \ldots q_p$, i.e. the flows of all previous and subsequent edges along $\tilde{\mathcal{P}}$, then q_i can have any value in the range $q_{i-1} > q_i > q_{i+1}$. If i is the first (last) edge along the path then it instead holds that $q_i > q_{i+1}$ ($q_i > 0$).

Proof. Assume edge *i* leads from some node *n* to some node *m* and consider equation (1), evaluated in nodes *n* and *m* respectively.

$$0 = q_{i-1} - q_i - q_n \tag{26}$$
$$0 = q_i - q_{i+1} - q_m \tag{27}$$

The signs are dictated by all edges being directed away from α. q_n and q_m are the sum of the flows in all edges directed away from nodes *n* and *m* respectively which are not part of the considered path. Due to the assumption that each internal node has at least degree 3, q_n and q_m must exist. As q_n and q_m are sums of some components of the boundary edge flows $\mathring{q}$, where Proposition 1 showed that any $\mathring{q} > 0$ is a viable, any $q_n > 0$, $q_m > 0$ are viable. This, along with a rearrangement gives that any

$$q_{i-1} - q_i > 0 \tag{28}$$
$$q_i - q_{i+1} > 0 \tag{29}$$

is viable, and simply correspond to different configurations of boundary flows. If *i* is the first (last) edge of the path, then only (28) (or (29)) applies. □

If (25) would hold, it implies that q_i as analyzed in Proposition 2 is a function of the other flows along the path. However, as Proposition 2 states, there is no such function but rather q_i can take any value within a range. The only conclusion is thus that $\lambda_e = 0$ for all e.

Section 4.2 shows that there is no λ where $\lambda_v \neq 0$ for any $v \in \mathring{\mathcal{E}}$ such that (21) holds in general. This section showed that there is no $\lambda_e \neq 0$ for any $e \in \bar{\mathcal{E}}$ such that (21) holds in general. This leads to the conclusion that the only solution to (21) is $\lambda = 0$. If load conditions are not sampled with some bias, it is therefore likely that the conditions of Theorem 1 should hold, especially if the number of load conditions T is large.

5. Numerical Example

A numerical example is now presented using a given network topology. Resistance parameter estimates $\hat{s}$ are computed and analyzed based on both noise-free and noisy measurement data. First a specific choice of f is provided.

5.1 District Heating Models

We consider a district heating model example where all edges e in the supply-and-return networks are pipes. They are described by pressure-relations

$$f(q_e, 1) \cdot s_e = q_e|q_e| \cdot \frac{2 f_{d,e} \rho L}{\pi^2 D_e^5}, \tag{30}$$

where $f_{d,e}$ is the Darcy friction factor, ρ is the density of the water, L is the length of the pipe and D_e is the diameter of the pipe, all assumed to be constant in time and and along the length of the pipe.

All boundary edges are control valves in customer substations, regulating the flow of hot water these customers receive. Control valves v have different characteristics in their mapping from valve position u_v to flow rate q_v at a given differential pressure. In district heating substations, this characteristic is often linear as stated in [Frederiksen and Werner, 2013]. We express this as

$$f(q_v, u_v) \cdot s_v = \frac{q_v|q_v|}{u_v^2} \cdot \frac{1}{k_v^2} \tag{31}$$

for valve v with valve setting u_v, where k_v is a linear parameter for the relation between flow and valve position.

5.2 Example Network

The example network under consideration is shown in Figure 2. This is the same network topology as was considered in [Liu et al., 2020], but now with added boundary edges and return network. Edges 1-6 are valves and edges 7-28 are pipes.

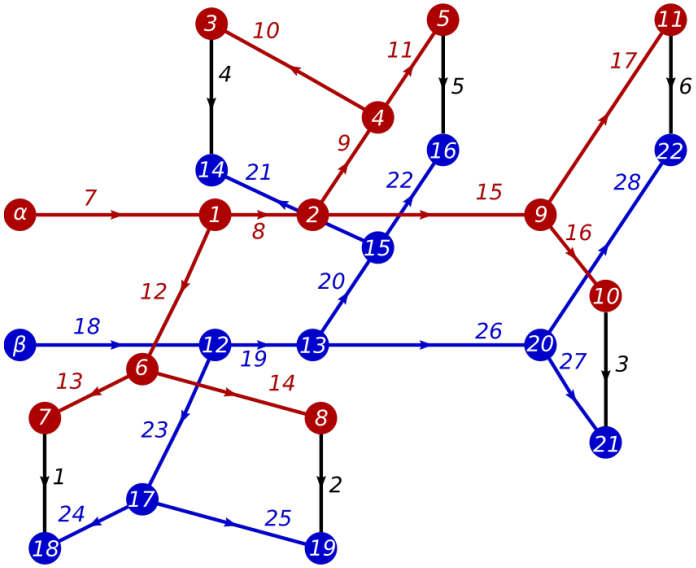

Figure 2. Network used in the numerical example.

The load conditions $t = 1 \dots T$ used in the numerical examples are generated the following way:

1. A set of boundary-flows $\mathring{q}(t)$ are sampled uniformly in the range $[100, 200]$.
2. Supply-network flows $\bar{q}(t)$ are calculated through (4).
3. The pressure drop in each supply-network edge is calculated using (30).
4. $p_\alpha - p_\beta$ is randomly selected sufficiently large such that (23) is feasible for all valves v.
5. The corresponding feasible valve positions u_v are calculated from (24).

Noisy measurements are considered. If x is a value generated by the above procedure, then the value used in the estimation process will be $\hat{x}$, sampled uniformly in the range $[x(1-\varepsilon), x(1+\varepsilon)]$ where ε denotes the noise level.

The deterministic case $\varepsilon = 0$ is considered first, followed by the noisy case $\varepsilon = 0.01$.

5.3 Deterministic Measurements

First we estimate the parameters using noise-free measurements under four load conditions. Table 1 presents the actual and estimated hydraulic parameters. Note

Table 1. Parameter values for each pipe and valve in the network. The estimated values $\hat{s}_i$ are rounded to 3 significant digits, and presented both without noise ($\varepsilon = 0.0$) and with noise $\varepsilon = 0.01$). Highlighted in bold and indexed with * are parameters where the supply-and-return edges have different parameter values.

Edge	s_i	$\hat{s}_i$, $\varepsilon = 0$	$\hat{s}_i$, $\varepsilon = 0.01$	
1	0.1	0.1	0.1	Valve
2	0.3	0.3	0.301	
3	0.2	0.2	0.199	
4	0.1	0.1	0.1	
5	0.4	0.4	0.401	
6	0.1	0.1	0.1	
7	0.0071	0.007	0.006	Supply-pipe
8	0.00028	0.0	0.0	
9*	**0.0767**	0.068	0.069	
10	0.54	0.54	0.538	
11	0.57	0.57	0.575	
12	0.031	0.031	0.031	
13	0.39	0.39	0.4	
14	0.7	0.7	0.693	
15*	**2.067**	1.828	1.835	
16	0.39	0.39	0.397	
17	0.64	0.64	0.627	
18	0.0071	0.007	0.006	Return-pipe
19	0.00028	0.0	0.0	
20*	**0.059**	0.068	0.069	
21	0.54	0.54	0.538	
22	0.57	0.57	0.575	
23	0.031	0.031	0.031	
24	0.39	0.39	0.4	
25	0.7	0.7	0.693	
26*	**1.59**	1.829	1.835	
27	0.39	0.39	0.397	
28	0.64	0.64	0.627	

that the pipe pairs 9-20 and 15-26 differ in parameters between supply and return, contrary to the assumptions of this paper. All parameters are estimated accurately except for these pairs. Note however, that $\hat{s}_9 + \hat{s}_{20} = s_9 + s_{20}$ and $\hat{s}_{15} + \hat{s}_{26} = s_{15} + s_{26}$. This is logical since this sum is utilized in reducing (12) to (13), which defines Φ. If as in [Wang et al., 2018] and [Liu et al., 2020] more pressure-measurements are available, individual parameters should be possible to estimate. However for many control applications such as [Agner et al., 2022], only the sum is required.

5.4 Noisy Measurements

Table 1 shows also the result of estimation when using $\varepsilon = 0.01$ (a maximum 1 % measurement error) and 100 load conditions. The parameters are still determined accurately.

Figures 3a and 3b show the confidence interval of the parameter estimates for edges 5 and 11 using increasing numbers of load conditions. For each point on the graphs, 1000 estimations are performed. These plots show that both for boundary edges and supply-side edges, the accuracy increases with the number of load conditions. In addition Figure 3c shows the boxplot of estimates using 50 load conditions, showing that all parameters are decided with reasonable accuracy, save for the previously discussed pairs 9-20 and 15-26 where instead the sum is accurate.

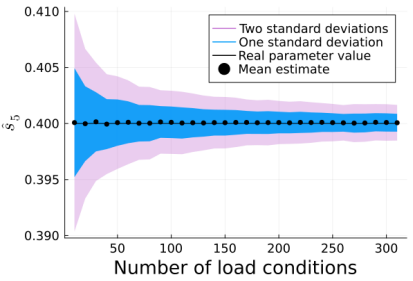

(a) Parameter confidence interval for edge 5, a boundary edge valve.

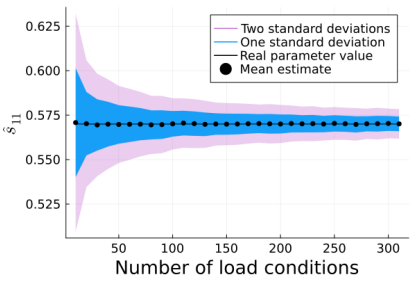

(b) Parameter confidence interval for edge 11, a supply network pipe.

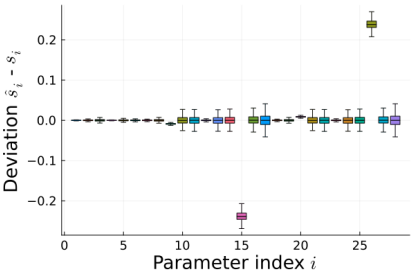

(c) Boxplot of parameter estimates for 50 load conditions.

Figure 3. Confidence interval progression for parameters 5 and 11 using increasing numbers of load conditions, as well as a boxplot of deviations from the real parameter value using 50 load conditions. Note that edge-pairs 9-20 and 15-26 are not centered, as these edges do not fulfill the assumption that return-and-supply pipes have equal parameter values. The boxplot and each point of the graphs are created using 1000 experiments each.

6. Conclusion

In this paper we showed how including a model of valve characteristics can be useful for identifying the hydraulic parameters of a district heating system, such that measurements of all pressures at customer substations are not needed. It was motivated how a set of equations, linear in the hydraulic parameters s, can be formed from operational data. A motivation was provided for why the solution s to these equations should be unique in practice. The resulting method was employed on a numerical example, where the estimation procedure was successful even under data gathered within a 1% measurement error.

6.1 Future Work

The function f in this numerical example does not fit all possible component characteristics. For instance, [Wang et al., 2018] consider *equal percentage* valves, rather than linear valves. In such a case, one can consider a kernel of functions $f_1, f_2, \ldots, f_n$, such that the pressure difference over each edge can be described as

$$p_n - p_m \approx f_1(q_e, u_e)s_{e,1} + f_2(q_e, u_e)s_{e,2} + \cdots + f_n(q_e, u_e)s_{e,n}. \quad (32)$$

More component types can be parameterized and considered. For instance, some boundary nodes could be by pumps, representing other producers in the network. Some of the edges in supply/return-networks could be booster pumps or valves.

Lastly, a generalization to meshed networks would be highly desirable. This is however difficult, as the linearity of the constraints (17) are based on calculating all edge flows explicitly.

References

Agner, F., P. Kergus, R. Pates, and A. Rantzer (2022). "Combating district heating bottlenecks using load control". *Smart Energy* **6**, p. 100067. ISSN: 2666-9552. DOI: https://doi.org/10.1016/j.segy.2022.100067.

Brange, L., K. Sernhed, and M. Thern (2019). "Decision-making process for addressing bottleneck problems in district heating networks". en. *International Journal of Sustainable Energy Planning and Management* **20**, pp. 37–50.

Frederiksen, S. and S. Werner (2013). *District heating and cooling*. Studentlitteratur. Chap. 2.

Liu, Y., P. Wang, and P. Luo (2020). "Pipe hydraulic resistances identification of district heating networks based on matrix analysis". *Energies* **13**:11. ISSN: 1996-1073. DOI: 10.3390/en13113007.

Lund, H., P. A. Østergaard, M. Chang, S. Werner, S. Svendsen, P. Sorknæs, J. E. Thorsen, F. Hvelplund, B. O. G. Mortensen, B. V. Mathiesen, C. Bojesen, N. Duic, X. Zhang, and B. Möller (2018). "The status of 4th generation district heating: research and results". *Energy* **164**, pp. 147–159. ISSN: 0360-5442. DOI: https://doi.org/10.1016/j.energy.2018.08.206.

Savic, D. A., Z. S. Kapelan, and P. M. Jonkergouw (2009). "Quo vadis water distribution model calibration?" *Urban Water Journal* **6**:1, pp. 3–22. DOI: 10.1080/15730620802613380. eprint: https://doi.org/10.1080/15730620802613380.

Vandermeulen, A., B. van der Heijde, and L. Helsen (2018). "Controlling district heating and cooling networks to unlock flexibility: A review". en. *Energy* **151**, pp. 103–115. ISSN: 03605442. DOI: 10.1016/j.energy.2018.03.034. URL: https://linkinghub.elsevier.com/retrieve/pii/S0360544218304328 (visited on 2021-07-14).

Wang, N., S. You, Y. Wang, H. Zhang, Q. Miao, X. Zheng, and L. Mi (2018). "Hydraulic resistance identification and optimal pressure control of district heating network". *Energy and Buildings* **170**, pp. 83–94. ISSN: 0378-7788. DOI: https://doi.org/10.1016/j.enbuild.2018.04.003.

Wang, Y., S. You, H. Zhang, W. Zheng, X. Zheng, and Q. Miao (2017). "Hydraulic performance optimization of meshed district heating network with multiple heat sources". *Energy* **126**, pp. 603–621. DOI: 10.1016/j.energy.2017.03.044.

Yin, G., B. Wang, T. Sheng, H. Sun, Q. Guo, and Z. Qiao (2018). "Network parameter estimation for district heating system". In: *2018 2nd IEEE Conference on Energy Internet and Energy System Integration (EI2)*, pp. 1–6. DOI: 10.1109/EI2.2018.8582515.